Western Tethys Early and Middle Jurassic calcareous nannofossil biostratigraphy

Jorge Ferreira[a], Emanuela Mattioli[a,b,*], Baptiste Sucherás-Marx[c], Fabienne Giraud[d], Luis V. Duarte[e], Bernard Pittet[a], Guillaume Suan[a], Auguste Hassler[a], Jorge E. Spangenberg[f]

[a] *Université de Lyon, UCBL, ENSL, CNRS, LGL-TPE, Villeurbanne 69622, France*
[b] *Institut Universitaire de France, Paris, France*
[c] *Aix Marseille Univ, CNRS, IRD, INRA, Coll France, CEREGE, Aix-en-Provence, France*
[d] *Université Grenoble Alpes, ISTerre, Grenoble F-38041, France*
[e] *MARE - Marine and Environmental Sciences Centre, Faculty of Sciences and Technology, Department of Earth Sciences, University of Coimbra, Portugal*
[f] *Institute of Earth Surface Dynamics (IDYST), University of Lausanne, Building Géopolis, Lausanne CH-1015, Switzerland*

A B S T R A C T

An exhaustive biostratigraphic study based on the calcareous nannofossil content from Lower and Middle Jurassic Lusitanian Basin sections in Portugal is here presented. Located at the strategic intersection of important Jurassic water masses during a period of drastic environmental changes, the Lusitanian Basin conveyed mixed phytoplanktonic communities in its surface waters. Approximately 800 m of exceptionally continuous Lower and Middle Jurassic series bearing detailed ammonite biostratigraphy and two Global Stratotype Section and Point are studied. Vertical and lateral ubiquity of calcareous nannofossils in marine sediments and rapid evolutionary rate and radiation make this fossil group a remarkable biostratigraphic tool. Nearly 100 bioevents are acknowledged in ~24 Myr time span this work refers to, bridging 11 nannofossil zones and 29 subzones. A thorough revision of the existing literature referring to Early and Middle Jurassic calcareous nannofossil biostratigraphy is presented, and causes and implications for zonal marker discrepancies discussed under a palaeoceanographic and Jurassic nannofossil evolution angle. In order to create a solid biostratigraphic frame and to compare it with C and O stable isotopic trends, brachiopod calcite shells were analysed for geochemistry. This work yields for the first time a very detailed and inclusive biostratigraphic scheme for the Early and Middle Jurassic epochs.

1. Introduction

During the Jurassic period, profound climatic and environmental changes deeply impacted the biosphere. The earliest Mesozoic oceanic anoxic event occurred during the Toarcian (T-OAE; Jenkyns, 1988) and relates to a hyperthermal event at ~182 Ma (Suan et al., 2008, 2010; Dera et al., 2011a) that was later followed by other periods of increased seawater temperature during the late Oxfordian-early Tithonian (e.g., Dera et al., 2011a; Zàk et al., 2011). Such climatic disruptions have been related accordingly to prolonged magmatic activity in the Karoo-Ferrar and Asian igneous provinces (Wang et al., 2006; Jourdan et al., 2007). On the other hand, episodes of marked cooling possibly associated with the temporary development of ice caps, took place during the late Pliensbachian, early Aalenian, Bajocian-Bathonian, and Callovian-Oxfordian (e.g., Jones et al., 1994; Price, 1999). Sea level drops

likely produced physical barriers within the complex high and low western Tethys seabed topography, changing the main currents circulations (Reggiani et al., 2010). The temporary development of marine anoxia also created chemical hurdles to organism migrations. Such barriers are most likely at the origin of the marked palaeoprovincialism observed in Jurassic ammonites (Macchioni and Cecca, 2002; Dommergues et al., 2009; Dera et al., 2011b), dinoflagellates (Bucefalo Palliani and Riding, 2003), foraminifera (Ruban and Tyszka, 2005), ostracods (Arias, 2007) and calcareous nannofossils (Bown, 1987; Mattioli et al., 2008).

The Jurassic Period chronostratigraphic framework is largely established through ammonite biostratigraphy. However, an alternative biochronological scheme based on a ubiquitous fossil group, able to rapidly and globally spread across water masses is needed since i) ammonites bear a marked provincialism, ii) the ammonite record in the
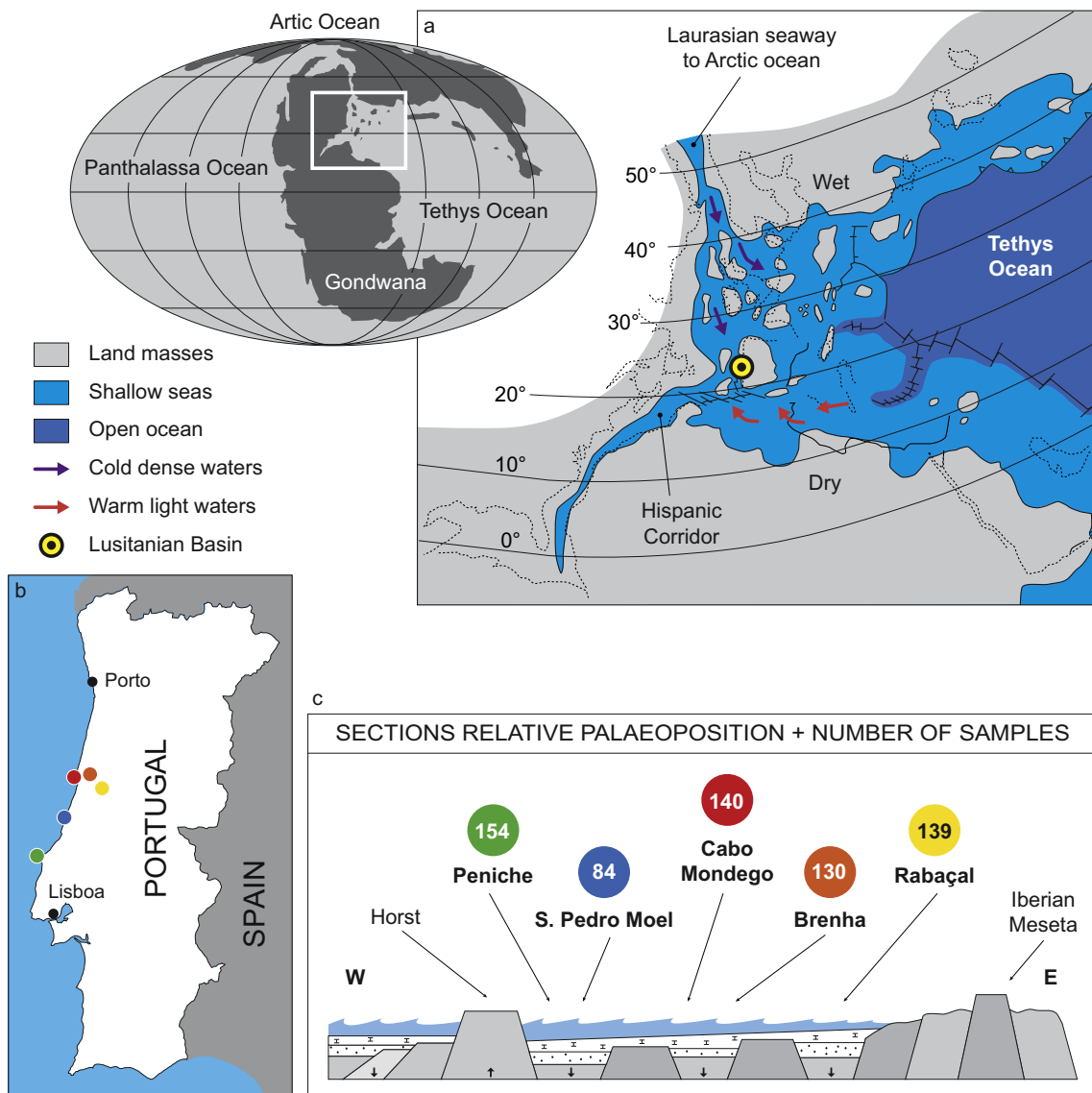
Fig. 1. (a) Western Tethys palaeogeography and location of the Lusitanian Basin within the proto-Atlantic rift during the Toarcian (modified after Bassoulet et al., 1993). (b) Location of the five studied sections in west Portugal, (c) their relative cross-section palaeoposition and the number of samples studied in each one of them.

increasing number of studies from continental cores is scarce, iii) the number of sites studied outside the western Tethys (Tibet, Canada, Japan, South America) where the standard ammonite biozones have been defined, is growing. Calcareous nannofossils are such ubiquitous fossil group. They include unicellular planktonic algae - the coccolithophores - covered by minute calcite platelets - the coccoliths - that lock together form a coccosphere. Marine snow and the inclusion of coccolithophore in zooplankton faecal pellets are the main mechanisms conveying coccospheres and coccoliths to the seafloor (Steinmetz, 1994). The rapid evolution and radiation of these organisms during the Early and Middle Jurassic makes them excellent palaeoecological, palaeogeographic and biostratigraphic tools.

Located at the junction of the western Tethys, the proto-Atlantic, the Arctic Ocean via the Viking corridor and the Panthalassa Ocean via the Hispanic corridor (Fig. 1), the Lusitanian Basin held a strategic position during the Jurassic period, as it acted as a N-S migration pathway for several organisms (e.g., ammonites, Mouterde and Ruget, 1975; ostracods, Arias, 2007; calcareous nannofossils, Reggiani et al., 2010). The nannofossil content from its sedimentary record therefore echoes the sway of the original nannoplankton community. In this work, a new biostratigraphic zonation scheme based on calcareous nannofossil from west Portugal (Lusitanian Basin), where continuous Lower and Middle Jurassic successions occur, is presented. These sections are well dated by ammonite biostratigraphy and bear an exceptional record of calcareous nannofossils. Due to the outstanding outcrop conditions and excellent fossil recovery, two Global Stratotype Section and Point (GSSP) have been established in the Lusitanian Basin at the base of the Toarcian stage in the Peniche peninsula (Rocha et al., 2016) and at the base of the Bajocian stage in the Cabo Mondego area (Pavia and Enay, 1997). Moreover, astrochronology and chemostratigraphy (δ^{13}C, δ^{18}O, ^{87}Sr/^{86}Sr, TOC content; e.g., Rocha et al., 2016) have been established for specific time intervals. The nannofossil record is herein compared to previous studies, and a new C and O stable isotope profile measured from brachiopod shells presented. This work is the first go at comprehensively integrate biostratigraphy and stable C and O isotopes for Lower and Middle Jurassic series in west Tethyan successions, and at correlate sections belonging to different palaeogeographic contexts. It also represents a considerable step forward in establishing a high-resolution biochronological frame where palaeoceanographic events suggested by major shifts in C and O isotope values and evolutionary patterns are integrated.

2. Previous work

Most of the Jurassic calcareous nannofossil biostratigraphy studies have been carried out in NW European sections such as England and Germany (e.g., Bown, 1987; Bown et al., 1988; Bown, 1996), in Mediterranean Tethys sections (e.g., Cobianchi, 1992; Lozar, 1992, 1995; Mattioli and Erba, 1999) and North Africa (de Kaenel and Bergen, 1993; de Kaenel and Bergen, 1993). Despite over the past decade some studies have addressed the Tethyan calcareous nannofossil biostratigraphy (e.g., Aguado et al., 2008; Sandoval et al., 2012; Mattioli et al., 2013; Fraguas et al., 2018), since Bown and Cooper (1998) and Mattioli and Erba (1999) no new biozonation scheme has been suggested for Lower and Middle Jurassic series. Nonetheless, and although with limited Tethyan data, nannofossil biozonations had already been summarized by Bown (1996) and de Kaenel and Bergen (1996).

The first studies of Early Jurassic calcareous nannofossils in the Lusitanian Basin are from Hamilton (1977, 1979). Later, Bown (1987) and de Kaenel and Bergen (1993) studied the nannofossil content from the Portuguese Brenha section. Late Sinemurian to Callovian stages were studied by Bergen (unpublished data) and reported in the synthesis work of de Kaenel and Bergen (1996), and later in Bown and Cooper (1998). More recent studies carried out in the Iberian Peninsula addressed the Pliensbachian and Toarcian nannofossil biostratigraphy (Perilli, 2000; Perilli et al., 2004; Perilli and Duarte, 2006; Perilli et al., 2010; Mattioli et al., 2013; Fraguas et al., 2015, 2018). However, the taxonomy adopted by some of these authors is someway different to the one followed herein. Actually, biometric studies of Jurassic coccoliths such as those performed on the genera *Similiscutum/Biscutum* (de Kaenel and Bergen, 1993; Mattioli et al., 2004), *Lotharingius* (Mattioli, 1996; Fraguas and Young, 2011; Ferreira et al., 2017), *Crepidolithus* (Suchéras-Marx et al., 2010; Fraguas and Erba, 2010), *Discorhabdus* (López-Otálvaro et al., 2012) and *Watznaueria* (Giraud et al., 2006; Tiraboschi and Erba, 2010), resulted in a quantitative and partially revised taxonomy. Such a revision deeply impacts biostratigraphic studies and therefore the chronostratigraphic range of the redefined taxa should be precisely determined.

3. Geological settings

The Lusitanian Basin was a small and narrow North-South elongated basin, sitting on the western side of the Iberian Massif and west-bounded by several basement horsts. This basin was one of the several rift-related peri-Tethyan Mesozoic basins whose origin was linked to the opening of the Atlantic Ocean (e.g., Pinheiro et al., 1996; Alves et al., 2002). The rhythmic sedimentation of successive hemipelagic marlstone-limestone couplets occurred on a homoclinal low-energy marine carbonate ramp sloping westwards. On such a ramp, diverse palaeoenvironments were established, displaying gradual changes in lithology with increasing depth (e.g., Duarte, 2007; Silva et al., 2015a). This elongated and shallow epicontinental seaway was located along the proto-Atlantic rift and connected the western Tethys to the NW European basins, and probably to the Panthalassa Ocean through the Hispanic Corridor. Its maximum water depth probably did not exceed 200 m (Bjerrum et al., 2001). Mixing between high NW European and low Mediterranean latitude waters has been described by various authors and supported by the mixing of ammonite fauna, ostracods and calcareous nannofossils during the Early Jurassic (Mouterde and Ruget, 1975; Dommergues et al., 2009; Arias, 2007; Reggiani et al., 2010; Dera et al., 2011b; Ferreira et al., 2015). Located at a palaeolatitude comprised between 25 and 30˚N (Dercourt et al., 2000), the Lusitanian Basin would correspond to the transition between subtropical and temperate climatic belts.

During the Early and Middle Jurassic, approximately 1 km of carbonate sediments controlled by sea level changes and tectonics were accumulated in this basin (e.g., Kullberg et al., 2013; Azerêdo et al., 2014). This thick carbonate infill begins with marginal-marine and restricted marine facies in the earliest Sinemurian, which rapidly grades upwards in the latest Sinemurian into hemipelagic fossiliferous marly limestone series (including organic-rich facies with black shales), which characterize most of the Lower Jurassic (Duarte, 1997; Duarte et al., 2010, 2012; Silva et al., 2015a). Only the sedimentary record from the western edge of the basin extends to the Callovian stage (e.g., Azerêdo et al., 2003, 2014). Five main sections comprising a succession of ~800 m of sediments ranging from the late Sinemurian up to the early Bajocian have been analysed: the Peniche section located close to the Berlengas-Farilhões topographic high and São Pedro de Moel and Cabo Mondego sections located in the distal part of the basin (Fig. 1). The Brenha section occupies the intermediate position between the distal and proximal part, the latter here represented by the Rabaçal section. In all sections, macrofossils such as ammonites, brachiopods, belemnites, bivalves and some fossilized wood fragments are commonly found.

São Pedro de Moel section spans from the late Sinemurian to the early Pliensbachian (Oxynotum to Jamesoni Zone), and the Peniche section follows it suit from the early Pliensbachian to the early Toarcian (Jamesoni to Levisoni Zone). Although the Rabaçal section spans from the latest Pliensbachian up to the late Toarcian, only the lowest 42 m comprising the latest Pliensbachian to the earliest middle Toarcian (Polymorphum to Bifrons Zone) were studied for nannofossil analysis. The Brenha section corresponds to the latest early Toarcian to the early Aalenian, and no ammonite studies were ever carried out here. The Cabo Mondego section ranges from the late Toarcian to the early Bajocian (Speciosum to Humphriesianum Zone). All sections are correlated by means of lithostratigraphy and ammonite and nannofossil biostratigraphy (Fig. 2).

Sections from the Lusitanian Basin are exceptionally continuous, well-exposed and bear a detailed ammonite biostratigraphy (e.g., Mouterde, 1955; Phelps, 1985; Comas-Rengifo et al., 2013; Kullberg et al., 2013; Silva et al., 2015b; Henriques et al., 2016) allowing nannofossil events to be directly calibrated to the standard regional Jurassic biostratigraphy. Sediments from the São Pedro de Moel region are included in the Coimbra, Água de Madeiros and Vale das Fontes Formations, those from the Peniche region are included in the Água de Madeiros, Vale das Fontes, Lemede and Cabo Carvoeiro Formations, those from the Rabaçal region in the São Gião Formation, and the remaining successions from Brenha and Cabo Mondego regions within the São Gião and Cabo Mondego Formations (e.g., Duarte and Soares, 2002; Azerêdo et al., 2003).

4. Material and methods

4.1. Calcareous nannofossils

A total of 647 closely spaced samples (approximately every 1 m and in key intervals at a closer sample-spacing of 0.1–0.2 m) were analysed from the marlstone-limestone couplets from five western Portugal sections and scanned for calcareous nannofossils. The studied time interval spans across the Oxynotum (late Sinemurian) up to the Humphriesianum Zone (early Bajocian) thus representing a time span of ~24.36 Myr (193.81 to 169.45 Ma; Gradstein et al., 2012). The number of samples collected and analysed in each of the sections are as follow: São Pedro de Moel: 84; Peniche: 154, Rabaçal: 139, Brenha: 130, Cabo Mondego: 140 (Fig. 1). Sample spacing is an important issue in order to evaluate the consistency of recorded events in consecutive samples. In the Lusitanian Basin, cyclostratigraphy is available for the early/late Pliensbachian transition (Suchéras-Marx et al., 2010), and for the early Toarcian interval (Suan et al., 2008). For these two intervals, the sample spacing can be directly translated into time average. For the rest of the studied interval, the timescale of Gradstein et al. (2012) was used to approximate the time between consecutive samples (Supplementary Material). In the late Sinemurian to early Pliensbachian interval of the S. Pedro de Moel section the average spacing of samples is 0.8 m, which corresponds to a time average of ~70 kyr (see
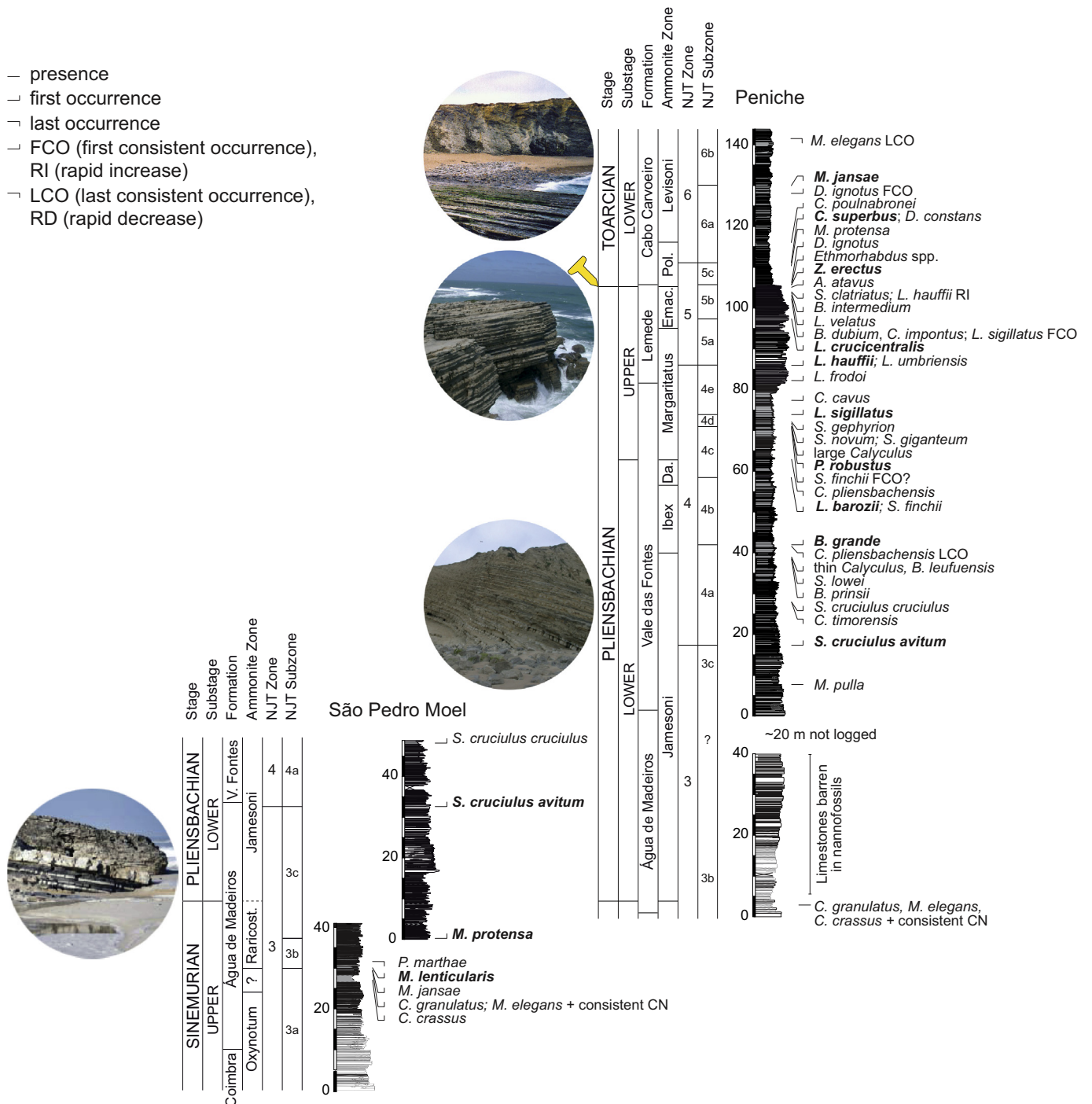
Fig. 2. Composite log of the five studied sections where ~100 nannofossil bioevents (FO, LO, FCO, LCO, RI, RD) recorded in ~24 Myr time span are plotted. Lithostratigraphy and ammonite biostratigraphy from Mouterde et al. (1955), Duarte and Soares (2002), Azerêdo et al. (2003) and Duarte et al. (2014). (a) Composite log of S. Pedro de Moel and Peniche sections. Raricos. = Raricostatum; Dav. = Davoei; Emac. = Emaciatum; Poly. = Polymorphum. Consistent CN: levels in which the record of calcareous nannofossils becomes consistent. (b) Composite log of Rabaçal, Brenha and Cabo Mondego sections. Poly. = Polymorphum; Bona. = Bonarelli; Specio. = Speciosum; Men. = Meneghinii; Aal. = Aalensis; Conca. = Concavum; Dis. = Discites; Hu. = Humphriesianum.

Supplementary Material). In the Pliensbachian of the Peniche section the average spacing of samples is 0.6 m, which corresponds to a time average of ~48 kyr. The close sample spacing we applied around the Pliensbachian/Toarcian boundary (0.1–0.2 m) allowed us to obtain a sample every 8–16 kyr, according to the cyclostratigraphic study by Suan et al. (2008). For the rest of early Toarcian, one sample per meter approximately corresponds to a time average of 60 kyr. Concerning the early Bajocian, the average sample spacing of 2.8 m corresponds to a time average of ~24 kyr.

Samples were prepared according to the method of Geisen et al. (1999) and nannofossils were studied under an optical polarized microscope with x1000 magnification. At least 450 fields of view corresponding to three slide transects were examined for each sample. On average 300 coccoliths were counted per sample as the counting of 300 specimens is statistically robust to record all the species making up > 1.7% of the total assemblage with a confidence level of 99.5% (Fatela and Taborda, 2002). Moreover, in all studied samples at least three extra transects were scanned in order to identify rare taxa and to
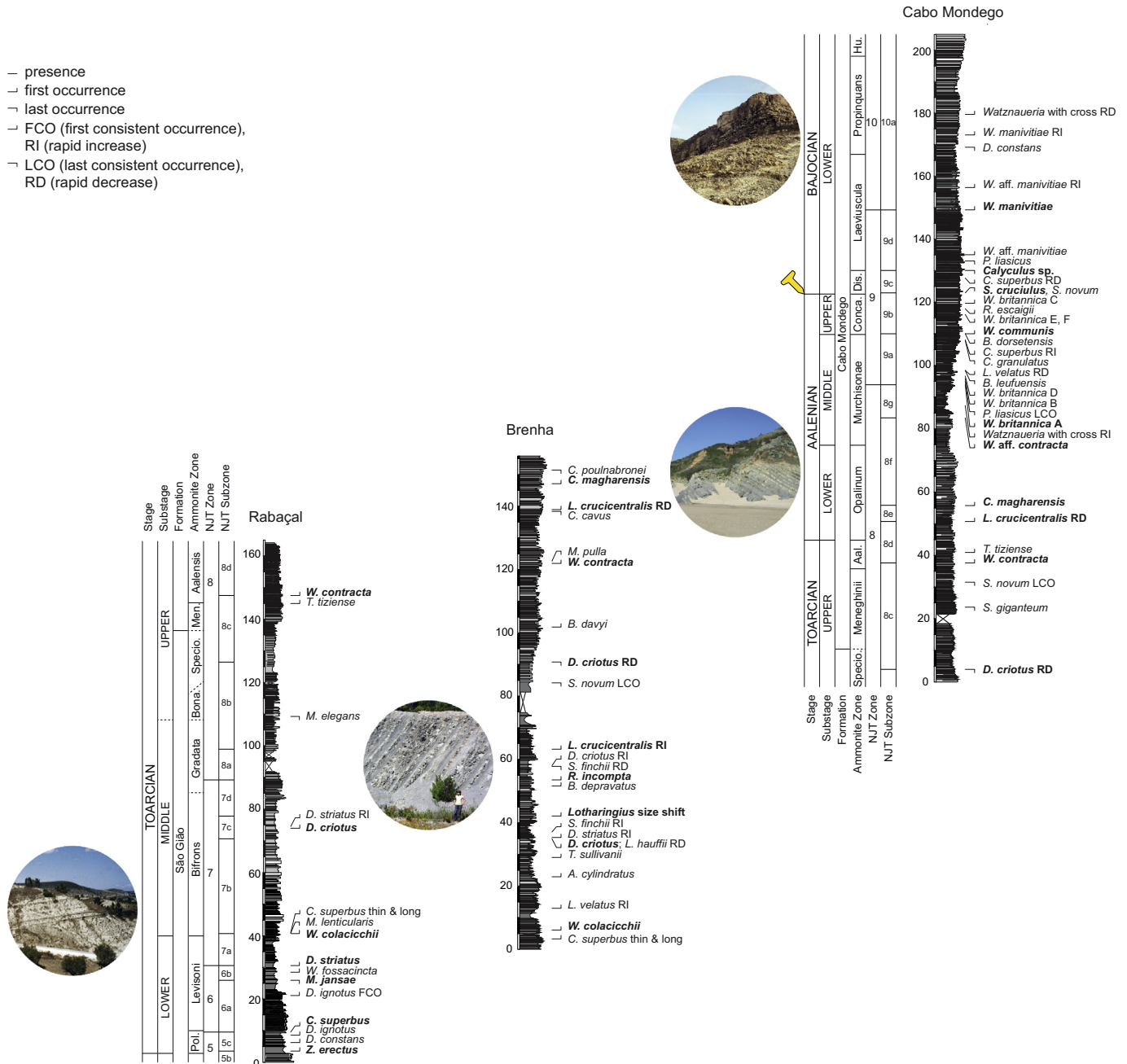
Fig. 2. (*continued*)

have a better record of the species richness. For each sample, species relative abundance was subsequently estimated from the total number of counted coccoliths so stratigraphic abundance changes could be easily perceived (see Supplementary Material). In order to achieve the highest possible counting accuracy, all samples were analysed at least twice within a year period. So as to avoid any taxonomic bias and to safeguard the same diagnostic criteria used in the species identification, all biostratigraphic markers and age-diagnostic taxa were scrutinized and blind tested among the present authors either through direct microscope viewing or through pictures.

Following Gradstein et al. (2012), the abbreviation FO (First Occurrence) is herein used for the first or stratigraphically lowest occurrence of a species in a section, LO (Last Occurrence) for the last or stratigraphically highest occurrence of a species in a section, FCO (First Consistent Occurrence) is used after a species is recorded in consecutive samples, LCO (Last Consistent Occurrence) after a species is no longer

observed in consecutive samples, and RI (Rapid Increase) for the stratigraphic horizon where a given taxa yields for the first time a relative abundance higher than 10% and maintain it throughout the subsequent samples. This is particularly suitable for dominant taxa such as the *Lotharingius* plexus in the Toarcian and the *Watznaueria* genus across the Aalenian and Bajocian stages. Conversely, RD (Rapid Decrease) is used for taxa that decrease their relative abundance to < 10% and maintain it. Biostratigraphy is described with reference to Bown and Cooper (1998) and Mattioli and Erba (1999). Calcareous nannofossil taxonomy follows that of Bown (1987) for muroliths, de Kaenel and Bergen (1993) and Mattioli et al. (2004) for *Similiscutum/Biscutum*, Mattioli (1996) and Ferreira et al. (2017) for *Lotharingius*, López-Otálvaro et al. (2012) for *Discorhabdus*, and Cobianchi et al. (1992), Mattioli (1996), Giraud et al. (2006) and Tiraboschi and Erba (2010) for *Watznaueria*. Since this study utilizes *Lotharingius* and *Watznaueria* species more frequently than previous biostratigraphic schemes, some

taxonomic keys to unambiguously differentiate these two genera are provided. Besides bearing diagenesis-resistant coccoliths, their use is appropriate as *Lotharingius* and *Watznaueria* species are dominant in Toarcian-Aalenian and Bajocian assemblages. Their use should thus guarantee that marker species can be easily recorded. Differences between these genera, both belonging to the Watznaueriaceae family, are referred by Cobianchi (1992) and Mattioli (1996). The latter provided some guidelines as the sutural lines among the elements of the distal shield (outer cycle) are more inclined in the coccoliths of the genus *Watznaueria* than in the genus *Lotharingius*, and the general shape of *Watznaueria* coccoliths being more concavo-convex. Such morphology renders an extinction pattern under optical microscopy where isogyres display right angle bent arms and a net optical discontinuity between outer and inner cycles of the distal shield. These characters are less obvious in the coccoliths of *Lotharingius* genus.

Calcareous nannofossil preservation was evaluated under optical microscopy according to their degree of etching, overgrowth and fragmentation. Generally, all coccoliths exhibited good (little or no evidence of dissolution nor overgrowth hence diagnostic traits were preserved allowing species-level identification) or moderate (although slightly altered by dissolution or overgrowth it was not enough to hamper species-level identification) preservation. Fragmentation was mainly observed in the *incertae sedis Schizosphaerella*.

4.2. Stable isotopes

A total of 47 brachiopod shells were analysed for their carbon and oxygen stable isotope composition. Fifteen of them were collected from the upper Sinemurian stage in São Pedro de Moel (Oxynotum and Raricostatum zones), and 32 from the middle Aalenian up to the lower Bajocian stages (Murchisonae up to Propinquans Zone) in Cabo Mondego. These new measurements were combined with previously published data from the Peniche (Hesselbo et al., 2007; Suan et al., 2010; Silva et al., 2011), Rabaçal (Ferreira et al., 2015) and Cabo Mondego (Suchéras-Marx et al., 2010) sections. The stable isotope profiles are a composite of different taxa of rhynchonellids, spiriferinids and terebratulids. Articulate brachiopods are assumed to be strictly benthic and commonly sessile organisms and it is considered that the oxygen isotope compositions of its fibrous inner calcite layer reflect the ocean water temperature and salinity (Suan et al., 2008; Brand et al., 2014). Conversely, the outer layer, which is considered to be secreted out of isotopic equilibrium with oceanic water in modern species (Carpenter and Lohmann, 1995; Auclair et al., 2003; Parkinson et al., 2005), was carefully removed with a dental scraper under a binocular microscope during sample preparation.

Stable carbon and oxygen isotope analyses were performed at the Institute of Earth Surface Dynamics of the University of Lausanne using a Thermo Fisher Scientific Gas Bench II carbonate preparation device connected to a Delta Plus XL isotope ratio mass spectrometer. The CO_2 extraction was done by reacting 100–200 μg of powdered rock with anhydrous phosphoric acid at 70 °C. The stable carbon and oxygen isotope ratios are reported in the delta (δ) notation as per mil (‰) deviation relative to the Vienna Pee Dee belemnite standard (VPDB). The standardization of the δ^{13}C and δ^{18}O values relative to the international VPDB scale was done by calibration of the reference gases and working standards with IAEA standards. Analytical uncertainty (1σ), monitored by replicate analyses of the international calcite standard NBS-19 and the laboratory standards Carrara Marble was not greater than ± 0.05‰ for δ^{13}C and ± 0.1‰ for δ^{18}O.

5. Nannofossil zonation and isotope excursions

Calcareous nannofossil bioevents recorded in this work are summarized in Fig. 3 and their FO, LO, RI, RD and FCO calibrated with the already established ammonite zones wherever they exist (see also Supplementary Material). In order to preserve the uniformity among different biozonation schemes, all zones and zone-defining criteria previously established by Bown and Cooper (1998) and Mattioli and Erba (1999) are kept. However, many subzones are emended here and new subzones introduced. Twenty-eight nannofossil subzones are recognized and hereafter scrutinized, 21 of which corresponding to new bioevents and defining new nannofossil subzones. All new subzones are established through easily recognizable index species (Plates 1 and 2), through diagenesis-resistant taxa even in diagenetically altered material, or species occurring synchronously amidst different successions. Each zonal marker or bioevent is examined in stratigraphic order from bottom to top. Whenever deemed necessary, taxonomy is discussed and findings compared to stratigraphic ranges already reported in the literature for both Mediterranean and Boreal palaeogeographic provinces. High-resolution sampling allowed to define whenever possible, nannofossil subzone horizons that match as closely as possible those of ammonites. Also, some nannofossil subzones closely correspond to stage boundaries, δ^{13}C positive or negative excursions or warming or cooling phases as indicated by the δ^{18}O record.

NJT3 - Crepidolithus pliensbachensis Zone

Defined by Mattioli and Erba (1999), this zone ranges from the FO of *Crepidolithus pliensbachensis* to the FO of *Similiscutum cruciulus*. It spans the late Sinemurian and early Pliensbachian (Jamesoni Zone) stage. In this work, the stratigraphic range of this zone matches the NJ3 Zone of Bown and Cooper (1998) and the NJT3 Zone of Mattioli and Erba (1999). Within this zone, a large number of species FOs occur, namely *Crepidolithus crassus*, *Crepidolithus granulatus*, *Mitrolithus elegans*, *Mitrolithus jansae*, *Mitrolithus lenticularis*, *Parhabdolithus marthae*, *Mazaganella protensa* and *Mazaganella pulla*.

NJT 3a - Crepidolithus pliensbachensis Subzone

Defined by Mattioli and Erba (1999), this subzone ranges from the FO of *Crepidolithus pliensbachensis* to the FO of *Mitrolithus lenticularis*. It spans the late Sinemurian, from the Oxynotum up to the basal Raricostatum Zone. This subzone partly corresponds to the NJ3 Zone of Bown and Cooper (1998) and the NJT3a Subzone of Mattioli and Erba (1999). Within this subzone occur the FOs of *C. crassus*, *C. granulatus*, *M. elegans* and *M. jansae*.

NJT 3b - Mitrolithus lenticularis Subzone

Defined by Mattioli and Erba (1999) and emended herein, this subzone ranges from the FO of *Mitrolithus lenticularis* to the FO of *Mazaganella protensa* (originally *Similiscutum cruciulus*). It spans the late Sinemurian within the Raricostatum Zone. This subzone partially corresponds to the NJ3 Zone of Bown and Cooper (1998) and the NJT3a Subzone of Mattioli and Erba (1999). Within this subzone occurs the LO of *P. marthae*. The reference section for this subzone is São Pedro de Moel.

NJT 3c - Mazaganella protensa Subzone

Defined herein, this subzone ranges from the FO of *Mazaganella protensa* to the FO of *Similiscutum cruciulus*. It spans the late Sinemurian and early Pliensbachian, from part of the Raricostatum up to part of the Jamesoni Zone. This subzone partially corresponds to the NJ3 Zone of Bown and Cooper (1998) and matches the NJT3b Subzone of Mattioli and Erba (1999). Although not a common taxon, its large size and tiered placoliths make the genus *Mazaganella* easily recognizable and resistent to dissolution. The reference section for this subzone is São Pedro de Moel. This subzone covers the Sinemurian/Pliensbachian boundary (Raricostatum/Jamesoni Zone) and records a prominent δ^{13}C negative excursion (Fig. 4).

NJT 4 - Similiscutum cruciulus Zone

Defined by Bown (1987) based of the FO of *Biscutum novum* (*B. novum* taxonomy was eventually emended; de Kaenel and Bergen, 1993; Mattioli et al., 2004) and emended by Bown and Cooper (1998). These authors considered the major evolutionary event of the FO of radiating placolith-coccoliths (i.e. *Similiscutum cruciulus*) for the base of this zone, as did Mattioli and Erba (1999). This zone ranges from the FO of *Similiscutum cruciulus* group to the FO of *Lotharingius hauffii*. It spans the early and late Pliensbachian, from part of the Jamesoni up to part of the

Fig. 3. Panel headers: Ma | Stages | Ammonite Zones | Nannofossil Zones and Subzones | Zonal markers (repeated for each of the three schemes).

This study

Stage	Ammonite Zones	Nannofossil Zones	Subzones	Zonal markers
BAJOC U/L	Parkinsoni, Garantiana, Niortense, Humphriesianum, Propinquans, Laeviuscula, Discites, Concavum	NJT11 / NJT10 / NJT9	NJT10b, NJT10a, NJT9d, NJT9c, NJT9b, NJT9a	W. barnesiae*, C. superbus**, W. manivitiae, Calyculus, S. cruciulus, W. communis
AALENIAN M/L	Murchisonae, Opalinum	NJT8	NJT8g, NJT8f, NJT8e, NJT8d, NJT8c, NJT8b, NJT8a	W. britannica, W. aff. W. contracta, C. magharensis, L. crucicentralis RD, W. contracta, D. criotus RD
TOARCIAN U/M/L	Aalensis, Meneghinii, Speciosum, Bonarelli, Gradata, Bifrons, Levisoni, Polymorphum, Emaciatum	NJT7, NJT6, NJT5	NJT7d, NJT7c, NJT7b, NJT7a, NJT6b, NJT6a, NJT5c, NJT5b, NJT5a	L. crucicentralis RI, R. incompta, Lotharingius size shift, D. criotus, W. colacicchii, D. striatus, M. jansae, C. superbus, Z. erectus, L. crucicentralis
PLIENSBACHIAN U/L	Margaritatus, Davoei, Ibex, Jamesoni	NJT4	NJT4e, NJT4d, NJT4c, NJT4b, NJT4a	L. hauffii, L. sigillatus, P. robustus, L. barozii, B. grande, S. cruciulus
SINEMUR U	Raricostatum, Oxynotum	NJT3	NJT3c, NJT3b, NJT3a	M. protensa, M. lenticularis

Mattioli & Erba, 1999

Ammonite Zones	Nannofossil Zones	Subzones	Zonal markers
Parkinsoni, Garantiana, Subfurcatum, Humphriesianum, Sauzei, Laeviuscula, Discites, Concavum	NJT10 / NJT9	NJT10b, NJT10a	C. superbus, W. manivitiae, W. britannica
Murchisonae, Opalinum	NJT8	NJT8c, NJT8b, NJT8a	C. margerelii, W. contracta, R. incompta
Aalensis, Pseudoradiosa, Insigne, Thouarsense, Variabilis, Bifrons, Serpentinus	NJT7, NJT6	NJT7b, NJT7a	D. criotus, D. striatus
Tenuicostatum, Spinatum, Margaritatus, Stokesi, Davoei, Ibex, Jamesoni	NJT5, NJT4	NJT5b, NJT5a, NJT4b, NJT4a	C. superbus, L. sigillatus, L. hauffii, P. robustus, S. cruciulus
Raricostatum, Oxynotum	NJT3	NJT3b, NJT3a	M. lenticularis

Bown & Cooper, 1998

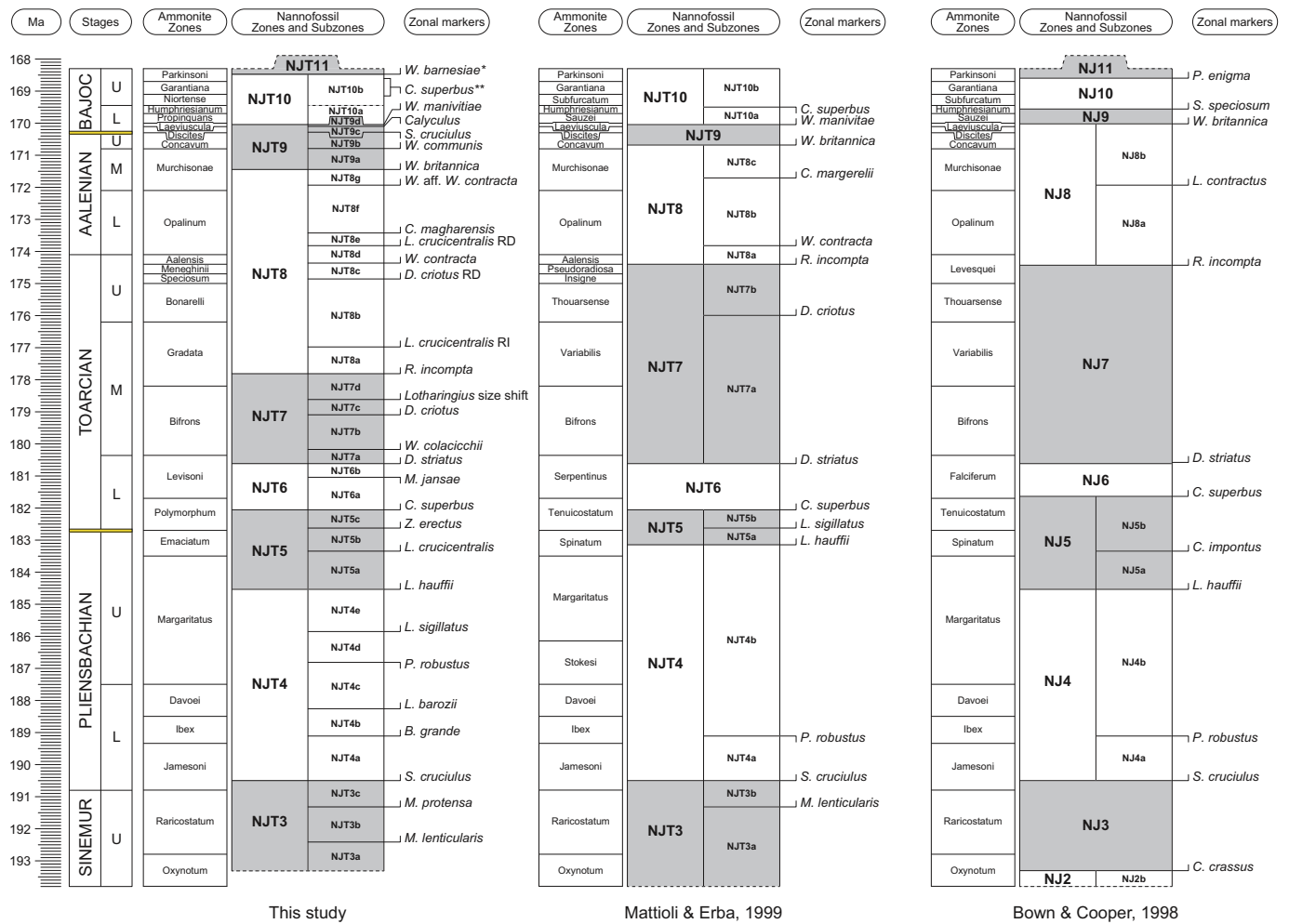| Ammonite Zones	Nannofossil Zones	Subzones	Zonal markers
Parkinsoni, Garantiana, Subfurcatum, Humphriesianum, Sauzei, Laeviuscula, Discites, Concavum	NJ11 / NJ10 / NJ9	NJ8b	P. enigma, S. speciosum, W. britannica
Murchisonae, Opalinum	NJ8	NJ8a	L. contractus
Levesquei, Thouarsense, Variabilis, Bifrons, Falciferum	NJ7, NJ6		R. incompta, D. striatus, C. superbus
Tenuicostatum, Spinatum, Margaritatus, Davoei, Ibex, Jamesoni	NJ5, NJ4	NJ5b, NJ5a, NJ4b, NJ4a	C. impontus, L. hauffii, P. robustus, S. cruciulus
Raricostatum, Oxynotum	NJ3, NJ2	NJ2b	C. crassus

Fig. 3. Nannofossil zonation defined for the Lusitanian Basin and its comparison with existing biozonation schemes covering the same time interval. Geochronology and ammonite zone durations after Gradstein et al. (2012), and ammonite biohorizons position have an error of ~100 kyr. (*) bioevent recorded by López-Otálvaro and Henriques (2018) in Cabo Mondego; (**) indicate the age interval where is predictable to observe the LO of *Carinolithus superbus*. The ammonite zonal markers used in Central Italy (Mattioli and Erba, 1999) and NW Europe (Bown and Cooper, 1998) are sometimes different from the Lusitanian Basin. Some discrepancies between zonal boundaries may occur in the different localities. See the text for more explanation.

Margaritatus Zone. This zone matches the NJ4 Zone of Bown and Cooper (1998) and partially corresponds to the NJT4 Zone of Mattioli and Erba (1999). Within this zone occur the FOs of *Similiscutum cruciulus cruciulus*, *Bussonius prinsii*, *Bussonius leufuensis*, *Sollasites lowei*, thin *Calyculus* sp., *Biscutum grande*, *Lotharingius barozii*, *Similiscutum finchii*, *Similiscutum novum*, *Similiscutum giganteum*, *Similiscutum gephyrion*, *Lotharingius sigillatus*, *Crepidolithus cavus*, *Lotharingius frodoi*. Within this zone also occur the LOs of *Crepidolithus timorensis*, *Parhabdolithus robustus* and *Crepidolithus pliensbachensis*. The reference section for this zone is Peniche.

NJT 4a - *Parhabdolithus robustus* Subzone

Defined by Mattioli and Erba (1999) and emended herein, this subzone ranges from the FO of *Similiscutum cruciulus* to the FO of *Biscutum grande* (originally the LO of *Parhabdolithus robustus*). It spans the early Pliensbachian, from part of the Jamesoni up to part of the Ibex Zone. This subzone corresponds to the NJ4a Subzone of Bown and Cooper (1998) and the NJT4a Subzone of Mattioli and Erba (1999). Within this subzone occur the FOs of *S. cruciulus cruciulus*, *B. prinsii*, *B. leufuensis*, *S. lowei*, the thin morphotype of *Calyculus* and also the LO of *Crepidolithus timorensis* and the LCO of *C. pliensbachensis*. The reference section for this zone is Peniche. The thin *Calyculus* morphotype is made up of elliptical coccoliths which in turn are made up of subvertical, juxtaposed elements. Its central area, which according to the genus diagnosis is filled with a grid (Noël, 1972), is not easily visible under
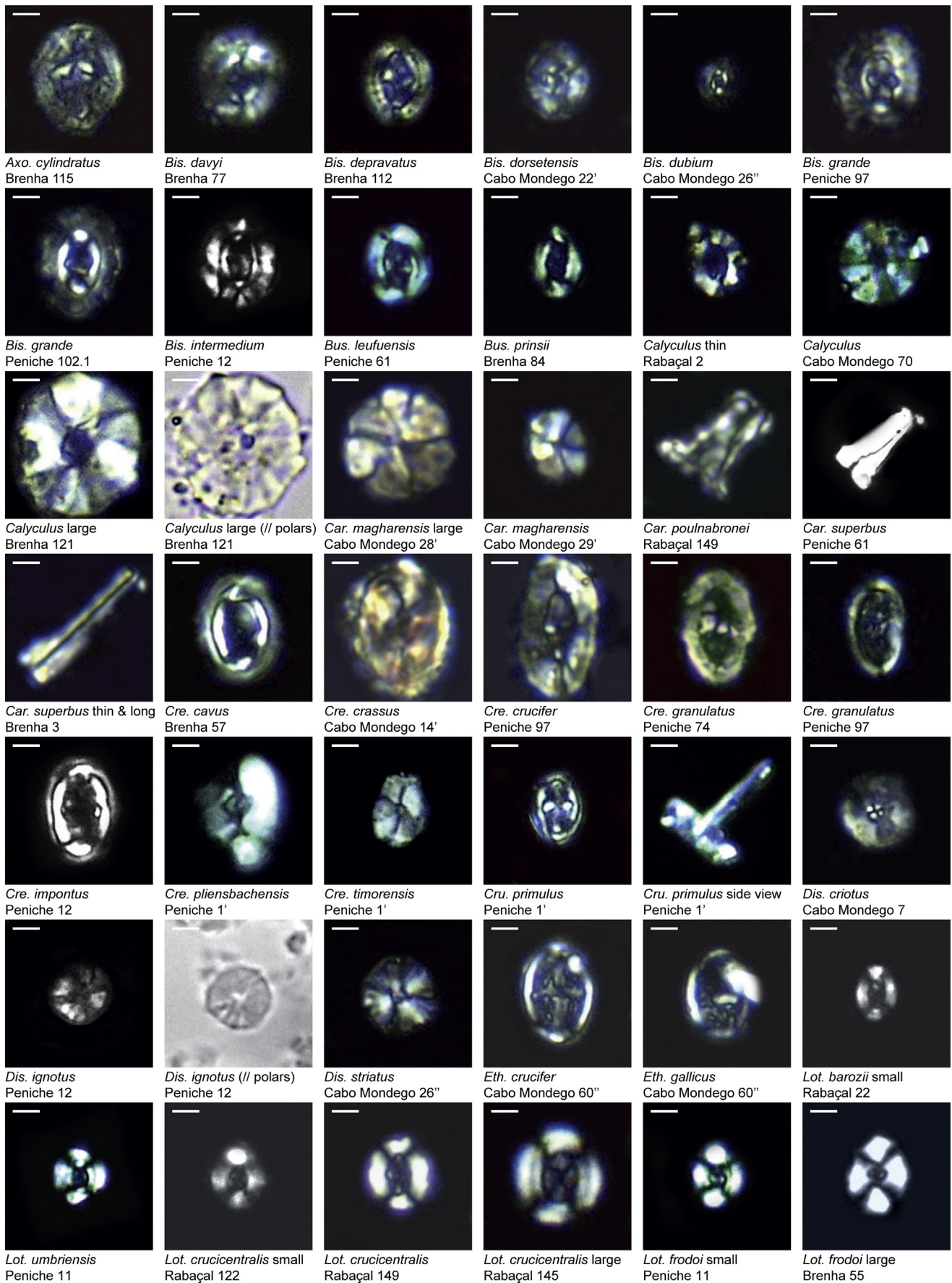
the optical microscope. The first appearance of this coccolith is a distinctive event, valuable in biostratigraphic studies.

NJT 4b - *Biscutum grande* Subzone

Defined herein, this subzone ranges from the FO of *Biscutum grande* to the FO of *Lotharingius barozii*. It spans the early Pliensbachian from part of the Ibex up to part of the Davoei Zone. This subzone partly corresponds to the NJ4b Subzone of Bown and Cooper (1998) and to the NJT4b Subzone of Mattioli and Erba (1999). The reference section for this subzone is Peniche. Due to its size, *Biscutum grande* is easily recognizable and resistant to dissolution making it a very useful index species.

NJT 4c - *Lotharingius barozii* Subzone

Defined herein, this subzone ranges from the FO of *Lotharingius barozii* to the LO of *Parhabdolithus robustus*. It spans the early and late Pliensbachian, from part of the Davoei up to part of the Margaritatus Zone. This subzone partially corresponds to the NJ4b Subzone of Bown and Cooper (1998) and to the NJT4b Subzone of Mattioli and Erba (1999). The FO of *S. finchii* happens synchronously with the FO of *L. barozii*, occurring both in the same sample. Within this subzone occurs the LO of *Crepidolithus pliensbachensis*. The reference section for this subzone is Peniche. The FO of *Lotharingius barozii* approximately defines the Ibex/Davoei Zone transition and represents the earliest occurrence of the *Lotharingius* genus, a group that will dominate the Early and Middle Jurassic assemblages. Noël (1973) first described *Lotharingius*

Axo. cylindratus
Brenha 115

Bis. davyi
Brenha 77

Bis. depravatus
Brenha 112

Bis. dorsetensis
Cabo Mondego 22'

Bis. dubium
Cabo Mondego 26''

Bis. grande
Peniche 97

Bis. grande
Peniche 102.1

Bis. intermedium
Peniche 12

Bus. leufuensis
Peniche 61

Bus. prinsii
Brenha 84

Calyculus thin
Rabaçal 2

Calyculus
Cabo Mondego 70

Calyculus large
Brenha 121

Calyculus large (// polars)
Brenha 121

Car. magharensis large
Cabo Mondego 28'

Car. magharensis
Cabo Mondego 29'

Car. poulnabronei
Rabaçal 149

Car. superbus
Peniche 61

Car. superbus thin & long
Brenha 3

Cre. cavus
Brenha 57

Cre. crassus
Cabo Mondego 14'

Cre. crucifer
Peniche 97

Cre. granulatus
Peniche 74

Cre. granulatus
Peniche 97

Cre. impontus
Peniche 12

Cre. pliensbachensis
Peniche 1'

Cre. timorensis
Peniche 1'

Cru. primulus
Peniche 1'

Cru. primulus side view
Peniche 1'

Dis. criotus
Cabo Mondego 7

Dis. ignotus
Peniche 12

Dis. ignotus (// polars)
Peniche 12

Dis. striatus
Cabo Mondego 26''

Eth. crucifer
Cabo Mondego 60''

Eth. gallicus
Cabo Mondego 60''

Lot. barozii small
Rabaçal 22

Lot. umbriensis
Peniche 11

Lot. crucicentralis small
Rabaçal 122

Lot. crucicentralis
Rabaçal 149

Lot. crucicentralis large
Rabaçal 145

Lot. frodoi small
Peniche 11

Lot. frodoi large
Brenha 55

(caption on next page)

Plate 1. Selected calcareous nannofossil micrographs. All micrographs are in crossed polars, except for the large *Calyculus* and *D. ignotus* (parallel polars). Different-sized morphotypes are shown for some species, in order to document the morphological variability observed in calcareous nannofossils from the Lusitanian basin. Scale bar is 2 μm.

←——

barozii from the Toarcian Schistes carton as a *Lotharingius* with massive buttresses in the axis of its ellipse and asymmetrical radial bars. According to Mattioli (1996; several sections) and the biometric study by Ferreira et al. (2017; sections in Portugal and France), this species is characterized by its elliptical shape with a narrow rim, a wide and elliptical central area spanned by an axial cross, and the inner and outer cycles of the distal shield have approximately the same thickness (Mattioli, 1996).

NJT 4d - *Similiscutum novum* Subzone

Defined herein, this subzone ranges from the LO of *Parhabdolithus robustus* to the FO of *Lotharingius sigillatus*. It spans the late Pliensbachian within the Margaritatus Zone. This subzone partially corresponds to the NJ4b Subzone of Bown and Cooper (1998) and to the NJT4b Subzone of Mattioli and Erba (1999). Within this subzone occur the FOs of the large morphotype of *Calyculus*, *S. novum*, *S. giganteum* and *S. gephyrion*. The reference section for this subzone is Peniche. The large morphotype of *Calyculus* recorded in this study is characterized by broadly elliptical distinctive coccoliths made up of sub-vertical, juxtaposed elements. These elements are thick, with a trapezoidal contour and thus rendering an irregular outline to the coccolith. Although impossible to determine at a species level when the diagnostic central area structures are not visible under optical microscope, the FO of this taxon seems to be a reliable event.

NJT 4e - *Lotharingius frodoi* Subzone

Defined herein, this subzone ranges from the FO of *Lotharingius sigillatus* to the FO of *Lotharingius hauffii*. It spans the late Pliensbachian within the Margaritatus Zone. This subzone partially corresponds to the NJ4b Subzone of Bown and Cooper (1998) and to the NJT4b Subzone of Mattioli and Erba (1999). Within this subzone occur the FOs of *C. cavus* and L. *frodoi*. The reference section for this subzone is Peniche. Although the earliest specimens of L. *sigillatus* recorded in this study being relatively small (4.34 μm on average for the upper Pliensbachian; Ferreira et al., 2017), its size increases throughout the Toarcian (5.14 μm on average; Ferreira et al., 2017). Stradner (1961) reported specimens of *Discolithus sigillatus* (basionym of L. *sigillatus*) as big as 6 to 8 μm from the middle Toarcian Variabilis Zone from SW Germany, but the emended diagnosis of Goy (1981) shows a holotype from the early Toarcian of 5 μm, which is very similar to those observed in this work. Mattioli (1996) first described L. *frodoi* as a small elliptical coccolith (average size of 3.5 μm during the earlier part of its stratigraphic range, up to 4.2 μm in the late Toarcian; Ferreira et al., 2017), with a narrowly elliptical central area, bearing two buttresses aligned with the minor axis of the ellipse.

NJT 5 - *Lotharingius hauffii* Zone

Defined by Bown (1987), this zone ranges from the FO of *Lotharingius hauffii* to the FO of *Carinolithus superbus*. It spans the late Pliensbachian and earliest Toarcian, from part of the Margaritatus up to part of the Polymorphum Zone. This zone partially corresponds to the NJ5 Zone of Bown and Cooper (1998), and to part of the NJT4 and whole NJT5 Zone of Mattioli and Erba (1999). A large number of FOs occur within this zone, namely of *Lotharingius umbriensis*, *Lotharingius crucicentralis*, *Biscutum dubium*, *Crepidolithus impontus*, *Lotharingius velatus*, *Axopodorhabdus atavus*, *Biscutum intermedium*, *Stradnerlithus clatriatus*, *Ethmorhabdus crucifer*, *Zeugrhabdotus erectus*, *Ethmorhabdus gallicus*, *Diductius constans* and *Discorhabdus ignotus*. Also, the LO of *Mazaganella protensa* and the RI of *Lotharingius hauffii* occur in this zone. The reference section for this zone is Peniche. Contrarily to previous evolutionary schemes presenting L. *hauffii* as the ancestor of all *Lotharingius* species (e.g., Cobianchi, 1992; Mattioli, 1996), the FO of L. *hauffii* is recorded in Portugal after those of L. *barozii* and L. *sigillatus*. *Lotharingius hauffii* is a small coccolith (on average in Portugal it is

≤ 4 μm), broadly elliptical to subcircular in shape, with a reduced central area. Its central area can sometimes be occupied by a knob or short spine. It is distinguishable from (1) *L. barozii* since the latter has a thin rim and a distinctive wide central area; (2) from L. *frodoi* as the latter is more elliptical in shape and possesses two buttresses in the central area (Mattioli, 1996); (3) from L. *sigillatus* because the latter is larger, more elliptical in shape and possesses an elongate central area with a longitudinal bar and a system of granular and radially disposed elements (Goy, 1981); (4) from L. *umbriensis* since the latter according to Mattioli (1996) is a small (3.5–5 μm), subcircular coccolith with a reduced central area filled by a small and distinctive cross.

NJT 5a - *Similiscutum finchii* Subzone

Defined by Mattioli and Erba (1999) and emended herein, this subzone ranges from the FO of *Lotharingius hauffii* to the FO of *Lotharingius crucicentralis* (originally *Lotharingius sigillatus*). It spans the late Pliensbachian across part of the Margaritatus up to the basal Emaciatum Zone. This subzone matches the NJ5a Subzone of Bown and Cooper (1998), and part of the NJT4b Subzone of Mattioli and Erba (1999). The reference section for this subzone is Peniche. The FO of L. *hauffii* and that of L. *umbriensis* are recorded synchronously, occurring both in the same sample. In this subzone, $\delta^{18}O$ values sharply increase thus suggesting an important cooling episode.

NJT 5b - *Lotharingius sigillatus* Subzone

Defined by Mattioli and Erba (1999) and emended herein, this subzone ranges from the FO of *Lotharingius crucicentralis* (originally *Lotharingius sigillatus*) to the FO of *Zeugrhabdotus erectus* (originally *Carinolithus superbus*). This subzone spans the topmost Pliensbachian within almost the totality of the Emaciatum Zone. It partially corresponds to the NJ5b Subzone of Bown and Cooper (1998), and matches the entire NJT5a Subzone of Mattioli and Erba (1999). Within this subzone occur the FOs of *B. dubium*, *C. impontus*, *L. velatus*, *A. atavus*, *B. intermedium* and *S. clatriatus*. Also, from the base of this subzone L. *sigillatus* is consistently recorded (FCO) and the RI of L. *hauffii* occurs. The reference section for this subzone is Peniche. *Lotharingius crucicentralis* (Medd, 1971) Grün and Zweili (1980) was first described in Oxfordian sections from Germany as a medium to large coccolith (8–13 μm), having a very distinctive cross in its wide central area. According to the biometric work by Ferreira et al. (2017), the size of this species in Portugal lies in the lower range of the type species in the Toarcian, being even smaller during the Pliensbachian. *Lotharingius velatus* is the latest species of the genus to occur in the uppermost part of the Pliensbachian stage and is characterized as being a broadly elliptical coccolith with a wide, oval central area filled by a granular plate (Bown and Cooper, 1989). Its average length in the Lusitanian Basin (Ferreira et al., 2017) closely matches that of the holotype (6.0 μm). The Margaritatus/Emaciatum Zone boundary roughly sits at the bottom of this subzone. Also, the Pliensbachian/Toarcian boundary and the coeval $\delta^{13}C$ negative excursion are included here.

NJT 5c - *Zeugrhabdotus erectus* Subzone

Defined herein, this subzone ranges from the FO of *Zeugrhabdotus erectus* to the FO of *Carinolithus superbus*. It spans the early Toarcian within the Polymorphum Zone. This subzone partially corresponds to the NJ5b Subzone of Bown and Cooper (1998), and equals the whole NJT5b Subzone of Mattioli and Erba (1999). Within this subzone occur the FOs of *E. gallicus*, *D. constans* and *D. ignotus*, the earliest of the *Discorhabdus* species and also the LO of *M. protensa*. The reference sections for this subzone are Peniche and Rabaçal. The birefringent transverse bar of *Zeugrhabdotus erectus* renders this species unequivocally recognizable. Although not a common species, its FO is of the utmost importance as this bioevent occurs close to the Pliensbachian/Toarcian boundary (Emaciatum/Polymorphum Zone) and is
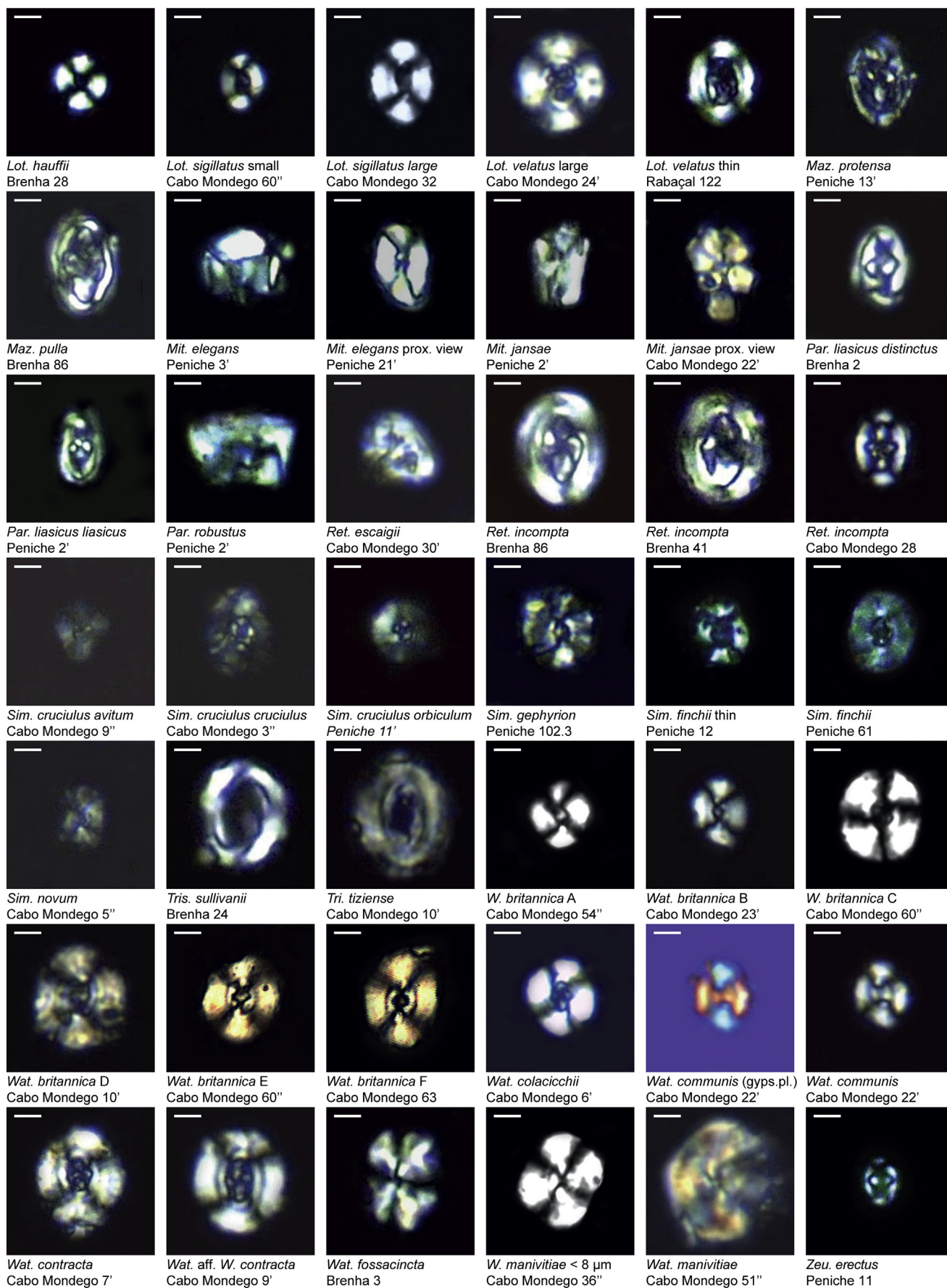
Plate 2. Selected calcareous nannofossil micrographs. All micrographs are in crossed polars, except for *W. communis* (gypsum plate). Different-sized morphotypes are shown for some species, in order to document the morphological variability observed in calcareous nannofossils from the Lusitanian basin. Scale bar is 2 μm.
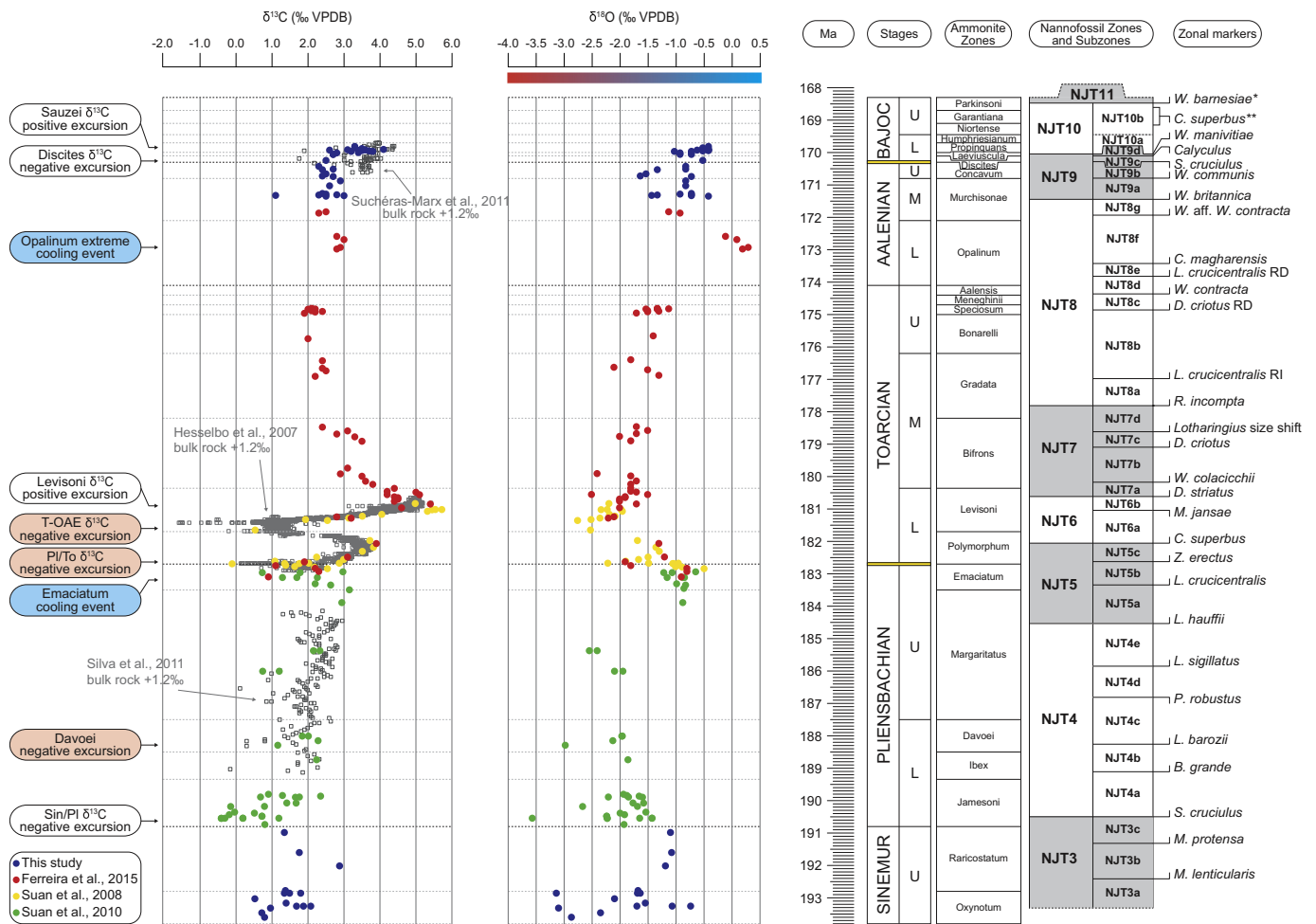
Fig. 4. Nannofossil zonation scheme and $\delta^{13}C_{brachiopod}$ plus $\delta^{18}O_{brachiopod}$ values across the Sinemurian-Bajocian stages. $\delta^{13}C_{bulk}$ is also shown according to published data. Note that the scale is the same as for $\delta^{13}C_{brachiopod}$, but the $\delta^{13}C_{bulk}$ curves are shifted by +1.2‰ units, which correspond to the original offset between the two sets of values (Suan et al., 2008). SINEMUR = Sinemurian; BAJOC = Bajocian.

synchronous in both distal and proximal sections, i.e. Peniche and Rabaçal. This subzone records the $\delta^{13}C$ positive rebound within the Polymorphum Zone.

NJT 6 - *Carinolithus superbus* Zone

Defined by Bown (1987), this zone ranges from the FO of *Carinolithus superbus* to the FO of *Discorhabdus striatus*. It spans the early Toarcian from part of the Polymorphum up to part of the Levisoni Zone. This zone partially corresponds to the NJ5 and the complete NJ6 Zone of Bown and Cooper (1998), and matches the entire NJT6 Zone of Mattioli and Erba (1999). Within this zone occurs the FO of *Carinolithus poulnabronei*, the *Watznaueria* genus, the LO of *Mitrolithus jansae* and the LCO of *M. elegans*. Also, in this zone is observed the FCO of *Discorhabdus ignotus*. The reference sections for this subzone are Peniche and Rabaçal. The earliest specimens of *Carinolithus superbus* recorded in the basal Toarcian have all the taxonomic features described by Deflandre and Fert 1954 for the holotype of *Rhabdolithus superbus*, although the inner wall connecting the proximal and distal shields is often in the lower range of the type species dimensions (10.3 μm in length, Deflandre and Fert 1954).

NJT 6a - *Carinolithus superbus* Subzone

Defined herein, this subzone ranges from the FO of *Carinolithus superbus* to the LO of *Mitrolithus jansae*. It spans the early Toarcian from part of the Polymorphum up to part of the Levisoni Zone. This subzone partially corresponds to the NJ5b Subzone and NJ6 Zone of Bown and Cooper (1998), and to part of the NJT6 Zone of Mattioli and Erba

(1999). Within this subzone occurs the FO of *C. poulnabronei* and the FCO of *D. ignotus*. The reference sections for this subzone are Peniche and Rabaçal. The $\delta^{13}C$ negative excursion commonly used to identify the Toarcian Oceanic Anoxic Event (T-OAE) sits within this subzone, and the sharp decrease in $\delta^{18}O$ values recorded in this subzone suggests a severe warming corresponding to the early Toarcian hyperthermal event.

NJT 6b - *Mitrolithus jansae* Subzone

Defined herein, this subzone ranges from the LO of *Mitrolithus jansae* to the FO of *Discorhabdus striatus*. It spans the early Toarcian within the Levisoni Zone. This subzone partially corresponds to the NJ6 Zone of Bown and Cooper (1998) and to the NJT6 Zone of Mattioli and Erba (1999). Within this subzone occurs the FO of *W. fossacincta*, the earliest of the *Watznaueria* species and the LCO of *M. elegans*. The reference sections for this subzone are Peniche and Rabaçal. This is a robust and synchronous event across the whole western Tethys. This subzone corresponds to the recovering period that follows the T-OAE where the highest $\delta^{13}C$ values are recorded (Fig. 4).

NJT 7 - *Discorhabdus striatus* Zone

Defined by Bown (1987), this zone ranges from the FO of *Discorhabdus striatus* to the FO of *Retecapsa incompta*. It spans the early and middle Toarcian, from the top of the Levisoni up to the basal Gradata Zone. This zone partially corresponds to the NJ7 Zone of Bown and Cooper (1998) and to the NJT7 Zone of Mattioli and Erba (1999). Because the FO of *R. incompta* is recorded at the basal Gradata Zone, the

top of NJT7 occurs far earlier than it was ever reported in the literature. Within this zone occur the FOs of *Watznaueria colacicchii* (the earliest *Watznaueria* with an axial cross in its central area), *Axopodorhabdus cylindratus*, *Triscutum sullivanii*, *Discorhabdus criotus*, *Biscutum depravatus* and the LO of *Mitrolithus lenticularis*. Also, the RD of *Lotharingius hauffii* occurs in this zone. The very long and thin morphotype of *C. superbus* (> 10 μm), easily detectable in optical microscope, also first occurs in this zone. Moreover, in this zone is also observed the RI of *Lotharingius velatus*, *Discorhabdus striatus* and *Similiscutum finchii* and the size shift of *Lotharingius* spp. with a mean size < 4 μm to > 4 μm. The reference sections for this zone are Rabaçal and Brenha. After returning to pre-excursion values, the δ^{13}C record enters a quite stable period that lasts until the end of the Toarcian, whereas δ^{18}O values start a steady positive drift that ends in the early Bajocian.

NJT 7a - *Discorhabdus striatus* Subzone

Defined by Mattioli and Erba (1999) and emended herein, this subzone ranges from the FO of *Discorhabdus striatus* to the FO of *Watznaueria colacicchii* (originally *Discorhabdus criotus*). It spans the early and middle Toarcian, from the topmost Levisoni up to the basal Bifrons Zone. This subzone partially corresponds to the NJ7 Zone of Bown and Cooper (1998) and to the NJT7a Subzone of Mattioli and Erba (1999). The reference section for this subzone is Rabaçal. *Discorhabdus striatus* can be differentiated from *D. ignotus* by its larger size (> 5 μm) and brighter birefringence colours (light grey) under polarizing light (López-Otálvaro et al., 2012).

NJT 7b - *Watznaueria colacicchii* Subzone

Defined herein, this subzone ranges from the FO of *Watznaueria colacicchii* to the FO of *Discorhabdus criotus*. It spans the middle Toarcian within the Bifrons Zone. This subzone partially corresponds to the NJ7 Zone of Bown and Cooper (1998) and to the NJT7a Subzone of Mattioli and Erba (1999). Within this subzone occur the FOs of *A. cylindratus* and *T. sullivanii*, the LO of *M. lenticularis*, and the enduring RI of L. *velatus*. The reference sections for this subzone are Rabaçal and Brenha. The FO of *Watznaueria colacicchii* is of paramount importance as it occurs at the lower/middle Toarcian boundary (Levisoni/Bifrons Zone) and is synchronous in both distal and proximal sections, i.e. Brenha and Rabaçal. This biostratigraphic marker should be easily recognizable as it is the first *Watznaueria* species with a relatively small and subelliptic central area filled by an axial cross. For being easily recognizable and bearing a consistent FO in south Tethyan sites, this bioevent is here deemed to be a strategic marker for the early/middle Toarcian boundary.

NJT 7c - *Discorhabdus criotus* Subzone

Defined herein, this subzone ranges from the FO of *Discorhabdus criotus* to the *Lotharingius* spp. size shift. It spans part of the middle Toarcian within the Bifrons Zone. This subzone partially corresponds to the NJ7 Zone of Bown and Cooper (1998) and to the NJT7a Subzone of Mattioli and Erba (1999). Within this subzone is observed the RI of *D. striatus* and *S. finchii*. Also, the RD of *Lotharingius hauffii* occurs in this subzone. The reference sections for this subzone are Rabaçal and Brenha. The name of this subzone was previously used by Mattioli and Erba (1999) for NJT7b.

NJT 7d - *Biscutum depravatum* Subzone

Defined herein, this subzone ranges from the *Lotharingius* spp. size shift to the FO of *Retecapsa incompta*. It spans the middle Toarcian from the top of the Bifrons to the basal Gradata Zone. This subzone partially corresponds to the NJ7 Zone of Bown and Cooper (1998) and to the NJT7a Subzone of Mattioli and Erba (1999). Within this subzone occurs the FO of *B. depravatus*. The reference section for this subzone is Brenha. The size increase of the *Lotharingius* genus is well defined and well recognizable in the middle Toarcian, differentiating early Toarcian assemblages dominated by small *Lotharingius,* from middle to late Toarcian assemblages characterized by large *Lotharingius* (Ferreira et al., 2017).

NJT 8 - *Retecapsa incompta* Zone

Defined by Bown et al. (1988) and emended by Mattioli and Erba

(1999), this zone ranges from the FO of *Retecapsa incompta* to the FO of *Watznaueria britannica*. It spans the middle Toarcian and middle Aalenian, from the basal Gradata up to the Murchisonae Zone. This zone partially corresponds to the NJ7 and NJT7, up to the NJ8 and NJT8 Zones of Bown and Cooper (1998) and Mattioli and Erba (1999). Within this zone occur the FOs of *Biscutum davyi*, *Watznaueria contracta*, *Triscutum tiziense*, *Carinolithus magharensis*, *Watznaueria* aff. *W. contracta* and the LOs of *Mitrolithus elegans*, *Similiscutum giganteum*, *Mazaganella pulla*, *Crepidolithus cavus* and *Carinolithus poulnabronei*. Moreover, in this zone is also observed the acme zone (RI and RD) of *Discorhabdus criotus* and *Lotharingius crucicentralis*, the RD of *Similiscutum finchii* and also the LCO of *Similiscutum novum*. The reference sections for this zone are Brenha and Cabo Mondego.

NJT 8a - *Retecapsa incompta* Subzone

Defined by Bown et al. (1988) and emended herein, this subzone ranges from the FO of *Retecapsa incompta* to the RI of *Lotharingius crucicentralis* (originally *Lotharingius contractus* syn. *Watznaueria contracta*; Cobianchi, 1992). It spans the middle Toarcian within the Gradata Zone. This subzone partially corresponds to NJ7 Zone of Bown and Cooper (1998) and to the NJT7a Subzone of Mattioli and Erba (1999). Within this subzone is observed the RD of *S. finchii* and the RI of *D. criotus*. The reference section for this zone is Brenha. The FO of *Retecapsa incompta* represents the earliest record of this species ever documented and can be used to approximately define the base of the Gradata Zone.

NJT 8b - *Lotharingius crucicentralis* RI Subzone

Defined herein, this subzone ranges from the RI of *Lotharingius crucicentralis* to the RD of *Discorhabdus criotus*. It spans the middle and late Toarcian, from part of the Gradata up to the basal Speciosum Zone. This subzone partially corresponds to the NJ7 Zone of Bown and Cooper (1998) and partially to NJT7a and NJT7b Subzones of Mattioli and Erba (1999). Within this subzone occurs the LCO of *S. novum*. The reference section for this subzone is Brenha.

NJT 8c - *Discorhabdus criotus* RD Subzone

Defined herein, this subzone ranges from the RD of *Discorhabdus criotus* to the FO of *Watznaueria contracta*. It spans the late Toarcian, from the Speciosum up to the basal Aalensis Zone. This subzone partially corresponds to the NJ7 Zone of Bown and Cooper (1998) and to the top NJT7b Subzone of Mattioli and Erba (1999). Within this subzone occur the FOs of *B. davyi* and *T. tiziense*, and also the LO of *S. giganteum*. The reference sections for this subzone are Brenha and Cabo Mondego.

NJT 8d - *Watznaueria contracta* Subzone

Defined herein, this subzone ranges from the FO of *Watznaueria contracta* to the RD of *Lotharingius crucicentralis*. It spans the late Toarcian and early Aalenian, from the basal Aalensis up to the basal Opalinum Zone. This subzone partially corresponds to the NJ8a Subzone of Bown and Cooper (1998) and to the NJT8a Subzone of Mattioli and Erba (1999). Within this subzone occur the LOs of *M. pulla* and *C. cavus*. The reference sections for this subzone are Brenha and Cabo Mondego. The FO synchronicity of *Watznaueria contracta* in both Cabo Mondego and Brenha sections renders this index species a robust marker for the Meneghinii/Aalensis Zone boundary. The name of this subzone was used by Bown (1988) to define the interval between the FO of *Lotharingius contractus* and the FO *Watznaueria britannica*. It was later emended by Mattioli and Erba (1999) who defined the *W. contracta* subzone from the FO of *W. contracta* and the FO of *Cyclagelosphaera margerelii*. Within this subzone lies the Toarcian/Aalenian boundary (Early/Middle Jurassic).

NJT8e - *Lotharingius crucicentralis* RD Subzone

Defined herein, this subzone ranges from the RD of *Lotharingius crucicentralis* to the FO of *Carinolithus magharensis*. It spans part of the early Aalenian within the Opalinum Zone. This subzone partially corresponds to the NJ8a Subzone of Bown and Cooper (1998) and to the NJT8b Subzone of Mattioli and Erba (1999). The reference sections for this subzone are Brenha and Cabo Mondego.

NJT8f - *Carinolithus magharensis* Subzone

Defined herein, this subzone ranges from the FO of *Carinolithus magharensis* to the FO of *Watznaueria* aff. *W. contracta*. It spans the early and middle Aalenian, from part of the Opalinum up to the basal Murchisonae Zone. This subzone partially corresponds to the NJ8a Subzone of Bown and Cooper (1998) and to the NJT8b Subzone of Mattioli and Erba (1999). Within this subzone occurs the LO of *C. poulnabronei*. The reference sections for this subzone are Brenha and Cabo Mondego. The FO of *C. magharensis* is of the utmost importance as it can be used to constrain the base of the Aalenian. The FO synchronicity of *C. magharensis* in both Cabo Mondego and Brenha sections makes this index species a robust early Aalenian marker, easily identifiable by its unmistakable hexagonal shape in distal view, made up of six triangular elements. Actually, up until now the FO of *C. magharensis* represented the most reproducible bioevent in the Mediterranean province for the basal Aalenian and was hence used in the definition of the GSSP of the Aalenian stage in the Fuentelsaz section (Cresta et al., 2001). $\delta^{18}O$ values reach their maxima within this subzone, thus indicating an extreme cooling event.

NJT8g - *Watznaueria* aff. *W. contracta* Subzone

Defined herein, this subzone ranges from the FO of *Watznaueria* aff. *W. contracta* to the FO of *Watznaueria britannica*. It spans the middle Aalenian within the Murchisonae Zone. This subzone roughly corresponds to part of the NJ8b Subzone of Bown and Cooper (1998) and to the NJT8c Subzone of Mattioli and Erba (1999). Within this subzone occurs the RI of *Watznaueria* spp. with a cross in its central area. The reference section for this subzone is Cabo Mondego. *Watznaueria* aff. *W. contracta* is easily identified for its large size (> 7 μm) and broadly elliptical central area filled with an axial cross, and can be used to approximately identify the early/middle Aalenian boundary (Opalinum/Murchisonae Zone).

NJT 9 - *Watznaueria britannica* Zone

Defined by Bown et al. (1988) and emended by Mattioli and Erba (1999), this zone ranges from the FO of *Watznaueria britannica* A, the earliest representative of the *W. britannica* plexus (i.e., *Watznaueria* with a bridge spanning across its central area) closely followed by the morphotypes B and D, to the FO of *Watznaueria manivitiae* (a *Watznaueria* with a closed central area and > 9 μm; Cobianchi, 1992). It spans the middle Aalenian and early Bajocian, from part of the Murchisonae up to part of the Laeviuscula Zone. This zone roughly corresponds to part of the NJ8 Zone of Bown and Cooper (1998) and to part of the NJT8 and entire NJT9 Zone of Mattioli and Erba (1999). Within this zone occur the FOs of all *Watznaueria britannica* morphotypes described by Giraud et al. (2006), *Biscutum dorsetensis*, *Watznaueria communis*, *Retecapsa escaigii*, *Watznaueria* aff. *W. manivitiae* (< 9 μm; Cobianchi et al., 1992) and the LOs of *Bussonius leufuensis*, *Crepidolithus granulatus*, *Similiscutum cruciulus*, *Similiscutum novum,* the large morphotype of *Calyculus* and *Parhabdolithus liasicus*. Moreover, in this zone is also observed the RD of *Lotharingius velatus* and the acme zone (RI and RD) of *Carinolithus superbus*. The reference section for this zone is Cabo Mondego. According to Reale et al. (1992) and Cobianchi (1992), *Watznaueria britannica* species were assigned to *Watznaueria* specimens possessing a bridge across their open central area. This bridge is parallel to the minor axis of the ellipse and is bright and optically-discontinuous with respect to the inner cycle of the coccolith rim under crossed-nicols. *Watznaueria britannica* varies considerably in coccolith size, opening of the central area, and shape of the bridge. Giraud et al. (2006) subdivided it into six morphotypes which are characterized as follows: 1) *W. britannica* A: small coccoliths (4.2 μm on average; Giraud et al., 2006), broadly elliptical to subcircular (length over ratio = 1.19), with an intermediate-sized central opening (26% of the coccolith) and a button-like bridge; 2) *W. britannica* B: medium-sized coccoliths (5.5 μm on average; Giraud et al., 2006), subelliptical (length over ratio = 1.23), with a small central opening (22% of the coccolith) and a button-like bridge; 3) *W. britannica* C: medium-sized coccoliths (5.3 μm on average; Giraud et al., 2006), broadly elliptical to

subcircular (length over ratio = 1.16), well-characterized by a wide, oval central opening (34% of the coccolith) transversely spanned by a distinctive thin bridge. This morphotype is the one resembling to the original diagnosis of *Coccolithus britannicus* by Stradner (1963); 4) *W. britannica* D: large coccoliths (7 μm on average; Giraud et al., 2006), subelliptical (length over ratio = 1.25), with a small-sized and subrectangular central opening (20% of the coccolith), and a thick bridge more or less parallel to the minor axis of the ellipse; 5) *W. britannica* E: medium to large coccoliths (6.1 μm on average; Giraud et al., 2006), subelliptical (length over ratio = 1.19), with a small-sized central opening (23% of the coccolith) and a rhombohedral bridge; 6) *W. britannica* F: medium-to-large coccoliths (6.1 μm on average; Giraud et al., 2006), narrowly elliptical (length over ratio = 1.3), with a very reduced central opening (14.5% of the coccolith) and a button-like bridge. Whatever the signification of these morphotypes (i.e., different species or ecophenotypes), they occur successively and represent important biostratigraphic events.

NJT 9a - *Watznaueria britannica* Subzone

Defined herein, this subzone ranges from the FO of *Watznaueria britannica*, with morphotype A, B, and D occurring one after the other, to the FO of *Watznaueria communis*. It spans the middle Aalenian within the upper half of the Murchisonae Zone. This subzone partially corresponds to the NJ8b Subzone of Bown and Cooper (1998) and to the NJT8c Subzone of Mattioli and Erba (1999). Within this subzone occurs the FO of *B. dorsetensis* and the LOs of *B. leufuensis* and *C. granulatus*. Moreover, in this subzone is also observed the RD of *L. velatus*, the RI of *C. superbus* and the LCO of *P. liasicus*. The reference section for this subzone is Cabo Mondego.

NJT 9b - *Watznaueria communis* Subzone

Defined herein, this subzone ranges from the FO of *Watznaueria communis* to the LO of *Similiscutum cruciulus*. It spans the whole late Aalenian and the Concavum Zone. This subzone partially corresponds to the NJ8b Subzone of Bown and Cooper (1998) and to part of the NJT8c and NJT9 Zone of Mattioli and Erba (1999). Within this subzone occur the FOs of *W. britannica* type C, E and F and *R. escaigii*. The reference section for this subzone is Cabo Mondego. *Watznaueria communis* is easily recognized by the optical continuum between its inner cycle and the thick bridge that crosses its central area (Cobianchi et al., 1992; Plate 2). Its FO is of the greatest importance as it closely defines the middle/late Aalenian boundary (Murchisonae/Concavum Zone). Despite its importance, this species has never been mentioned before in any biostratigraphic schemes or compilations. A minor but relevant bulk carbonate $\delta^{13}C$ negative excursion occurs in this subzone (Suchéras-Marx et al., 2012).

NJT 9c - *Biscutum dorsetensis* Subzone

Defined herein, this subzone ranges from the LO of *Similiscutum cruciulus* group to the LO of the large morphotype of *Calyculus*. It spans the early Bajocian within the totality of the Discites Zone. This subzone partially corresponds to the NJ8b Subzone of Bown and Cooper (1998) and to the NJT9 Zone of Mattioli and Erba (1999). In this subzone is observed the LO of *S. novum* and the RD of *C. superbus*. The reference section for this subzone is Cabo Mondego. The LO of *Similiscutum cruciulus* is of extreme importance as it lies at the Aalenian/Bajocian boundary (Concavum/Discites Zone). The disappearance of the small morphotypes of the genus *Similiscutum* in this subzone is pertinent, as these radiating placoliths were a major representative of Early Jurassic assemblages.

NJT 9d - *Calyculus* Subzone

Defined herein, this subzone ranges from the LO of the large morphotype of *Calyculus* sp. to the FO of *Watznaueria manivitiae*. It spans the early Bajocian within part of the Laeviuscula Zone. This subzone approximately matches the NJ8/NJ9 and NJT9/NJT10 Zone boundaries of Bown and Cooper (1998) and Mattioli and Erba (1999). Within this subzone occurs the FO of *W.* aff. *W. manivitiae* (< 9 μm) and the LO of *P. liasicus*. The reference section for this subzone is Cabo Mondego. The LO of the large *Calyculus* represents an important bioevent as it lies at

the Discites/Laeviuscula Zone boundary.

NJT 10 - *Watznaueria manivitiae* Zone

Defined by Reale et al. (1992) and emended by Mattioli and Erba (1999), this zone ranges from the FO of *Watznaueria manivitiae* to the FO of *Watznaueria barnesiae*. It spans the early and late Bajocian, from part of the Laeviuscula up to part of the Parkinsoni Zone. This zone approximately corresponds to the NJ9 and NJ10 Zone of Bown and Cooper (1998) and matches the NJT10 Zone of Mattioli and Erba (1999). Within this zone occurs the LO of *Diductius constans* and although the upper Bajocian stage was not sampled, it is in this interval that occurs the LO of *Carinolithus superbus*. Also in this zone are recorded the RIs of *Watznaueria* aff. *W. manivitiae* and *Watznaueria manivitiae*, and the RD of *Watznaueria* sp. with a cross. This zone records a distinct shift towards higher δ^{13}C values.

6. Discussion

6.1. Comparison with previous studies

First and last occurrence datums recorded in this study are plotted against the ammonite biozonation defined for the Lusitanian Basin, a region where exchanges between NW European and Mediterranean water masses occurred. However, the correlation of nannofossil bioevents and ammonite zones between other western Tethys basins is not always seamless due to the pronounced ammonite provincialism during the Early and Middle Jurassic (e.g., Macchioni and Cecca, 2002; Dommergues et al., 2009; Dera et al., 2011b). Though diachroneity between nannofossil events is often interpreted as due to poor preservation or palaeoprovincialism, bioevents bearing significant discrepancies are here scrutinized and possible causes for such inconsistencies debated.

6.1.1. Discrepancies due to ammonite stratigraphy

In Table 1, the comparison between ammonite zones associated with the bioevents used in this work for establishing biozones and that from the literature is presented. Reference nannofossil biostratigraphy papers for the NW Europe (Bown, 1987; Bown and Cooper, 1998) are based on numerous sections and boreholes in Europe, Portugal and offshore Morocco. However, a detailed ammonite zonation is only shown in these works for the Jurassic Mochras borehole and the Brenha section. Although ammonite zones for the Toarcian stage in NW Europe have all been recognized in the Mochras borehole (Ivimey-Cook, 1971; Copestake and Johnson, 2014), one may argue that the macrofossil record from a core is more fragmentary than in well-exposed outcrops like those from the Portuguese coast. As such, fragmentation may yield a degree of uncertainty with regard to ammonite zone boundaries. The same concern affects the boreholes studied in northern France by Peti et al. (2017) and in Germany by van de Schootbrugge et al. (2018). As for the Brenha section, it has already been studied by Hamilton (1977, 1979) and Bown (1987) and now the present work. However, no detailed work on ammonite biostratigraphy exists in the literature regarding this section. Apart from Brenha, all the other sections, hold a very accurate ammonite biostratigraphy that has been extensively studied since the Fifties (e.g., Mouterde, 1955; Phelps, 1985; Henriques et al., 2016). These sections bear a well-established ammonite stratigraphy, where two GSSP were defined: one at the base of the Toarcian stage in the Peniche peninsula (Rocha et al., 2016) and the other at the base of the Bajocian stage in the Cabo Mondego area (Pavia and Enay, 1997).

Apart from the aforementioned problem linked to the precision of ammonite zone definition, palaeoprovincialism may also have an impact on ammonite chronostratigraphy. The FO of *Carinolithus superbus* is a distinctive event. This species is easily identifiable due to its developed distal inner tube and its closed central area, granting it an unmistakable T-shape in side view. This species is easily distinguishable from its sibling *C. poulnabronei* since the distal shield of the latter holds

a slightly open central area and thus displays a V-shape in side view (Plate 1). The FO of *C. superbus* occurs during the δ^{13}C positive rebound, between the Pliensbachian/Toarcian boundary and the T-OAE δ^{13}C negative excursion. However, its FO is diachronous in the literature (Table 1), occurring either in the earliest or the second early Toarcian ammonite zone. As already mentioned, the Toarcian was an age of relevant ammonite provincialism that can be attested by the different zonal markers used in Mediterranean and NW European sections: Polymorphum versus Tenuicostatum for the earliest zone, and Levisoni versus Serpentinum or Falciferum for the latest zone (Fig. 3). In the literature, the first and second Toarcian ammonite zone are considered to be synchronous across the Mediterranean and the NW Europe provinces (e.g., Gradstein et al., 2012). However, based on the first appearance datums (FAD) of ammonite species, Macchioni and Cecca (2002) showed that the base of the Polymorphum Zone in the Mediterranean province predates the base of the Tenuicostatum Zone in NW Europe. Similarly, the base of the second Toarcian ammonite zone has been considered as potentially diachronous with regard to the δ^{13}C minimum record during the T-OAE (see figure 5 in Jenkyns et al., 2002, and Fig. 1 in Wignall et al., 2005). The difficulty of large-scale correlation for the second ammonite zone of the Toarcian has been widely debated by Macchioni (2002). Such difficulties bring heavy consequences for the correlation of organic matter enriched levels and the related T-OAE negative δ^{13}C excursion across Europe. Since it is now widely accepted that the early Toarcian negative δ^{13}C excursion is a global and synchronous event, and that the base of the *C. superbus* zone encapsulates the onset of this excursion, it is probable that the diachronism in the FO of *C. superbus* is only apparent and likely due to discrepancies in the ammonite record. In fact, in many Mediterranean sites such as the Valdorbia section in central Italy, the ammonite record is very scarce in the organic-rich interval, and the base of the Serpentinum Zone was placed in the interval above the negative δ^{13}C excursion of the T-OAE with some degrees of uncertainty (Sabatino et al., 2009).

6.1.2. screpancies due to taxonomic concepts

The most representative genera of Early and Middle Jurassic assemblages are *Lotharingius* and *Watznaueria*. Despite their abundance and dominance during the Toarcian/Aalenian and Bajocian/Oxfordian, the two genera have been largely underestimated in feature biozonation schemes (e.g., Bown and Cooper, 1998; Mattioli and Erba, 1999). This is mainly due to the existence of morphological continuums, which have hampered clear taxonomic subdivisions. As already mentioned, the development over the last decade of bio- and morphometric techniques and taxonomic revisions have led to significant advances in the discrimination between morphospecies, with an indirect but relevant impact in biochronology. The FO of *L. hauffii* (Table 1) illustrates such impact. The rare discrepancies found in the literature for this reliable bioevent at the top of the Margaritatus Zone are most likely due to its misidentification, as the presence of small *Lotharingius* morphospecies, such as *L. frodoi*, occurs earlier.

Another event worth using for biochronological purposes is the FO of *L. sigillatus*. In the literature, this bioevent appears to be quite diachronous (Table 1). However, this apparent diachronism is related to different taxonomic concepts used in its identification. In fact, all the specimens assigned here to *L. sigillatus* bear the taxonomic criteria typical of this species but are in the lower range of the holotype size. Ferreira et al. (2017) showed that all *Lotharingius* species are very small during the late Pliensbachian and increase significantly at the end of the middle Toarcian. Some authors though, only consider true *L. sigillatus* those specimens larger than 5 μm (de Kaenel, personal communication). The specimens of *L. sigillatus* recorded here in the Margaritatus Zone are often slightly smaller than 5 μm, although they show the diagnostic traits of this species. Another possible explanation for the observed discrepancies is likely related to a species discontinuous record after its FO. For instance, most of the FOs of *L. sigillatus* that are found in the

Table 1

Comparison between ammonite zones associated with bioevents used in this work, and feature literature Sandoval et al., 2008.

Zonal marker	Portugal				Morocco	Switzerland	NW Europe	Spain			central Italy	N France	Germany
	This work (includes Mattioli et al, 2013)	Hamilton, 1977; 1979	Perilli and Duarte, 2006	de Kaenel et al., 1996	de Kaenel et al., 1996	de Kaenel et al., 1989	Bown and Cooper, 1998	Perilli, 2000; Perilli et al., 2010	Fraguas et al., 2015'; 2018"	Aguado et al., 2008'; 2017"; Sandoval et al., 2008"'; 2012""	Mattioli and Erba, 1999	Peti et al., 2017	van de Schootbrugge et al., 2018
W. manivitiae	**laeviuscula**						mid Bathonian				**laeviuscula/sauzei**		
Calyculus LO	very base laeviuscula	bifrons					top sauzei			mid meneghinii"	top opalinum		
S. cruciulus LO	base discites						spinatum / tenuicostatum			top aalensis"	very top convcavum		
W. communis	**very base concavum**		not studied				base discites			**top concavum"'**	base discites		
W. britannica	mid murchisonae	tenuicostatum (3)			mid discites	mid discites	base laeviuscula			base discites"" (8)	very top concava	not studied	
W. aff. W. contracta	base murchisonae							not studied	not studied		mid discites		not studied
H. magharensis	**base opalinum**				**top opalinum**		levesquei / opalinum			**top opalinum' "'**	mid opalinum		
W. contracta	**base aalensis**		top aalensis		base opalinum	**very top aalensis**	base murchisonae			**base opalinum"' / mid aalensis""'**	base opalinum		
R. incompta	base gradata		base bonarelli	base pseudoradiosa	base opalinum	mid aalensis	top levesquei			base bradfordensis"	pseudoradiosa/ aalensis		
D. criotus	**mid bifrons**		top gradata	base variabilis	**top bifrons**	top variabilis	bifrons/variabilis			top bifrons""	mid thouarsense	**mid bifrons (9)**	
W. colacicchii	**base bifrons**									mid bifrons""	**top serpentinum**		
D. striatus	**top levisoni**		base bifrons	top bifrons	very top serpentinus	**top serpentinus**	very top falciferum	very top serpentinus		top serpentinum""	top serpentinum	top serpentinum (9)	mid bifrons
M. jansae LO	**mid levisoni**		**base levisoni**	base bifrons	very top serpentinus	very top tenuicostatum	very top falciferum	base serpentinus			top serpentinum	unzoned between tenuicostatum / serpentinum (9)	
C. superbus	mid polymorphum	tenuicostatum / falciferum	mid levisoni	mid bifrons	middle serpentinus	**base serpentinus**	**base falciferum**	mid serpentinus	**top tenuicostatum**	**base serpentinum""**	mid tenuicostatum	unzoned between tenuicostatum / serpentinum (9)	top serpentinum
Z. erectus	**very base tenuicostatum**	earlier than oxynotum (4)					spinatum / tenuicostatum					**very top spinatum**	
L. crucicentralis	mid emaciatum						tenuicostatum		spinatum	top emaciatum""	base tenuicostatum	mid margaritatus (10)	
L. hauffii	**top margaritatus (1)**			top margaritatus	top margaritatus	**very top margaritatus**	**mid margaritatus**	base margaritatus	base margaritatus' / mid margaritatus"		top emaciatum	**top margaritatus**	very top davoei (11)
L. sigillatus	mid margaritatus (2)	tenuicostatum / falciferum (5)			very top spinatum	very top tenuicostatum	base spinatum	base spinatum	base spinatum		top emaciatum	**top margaritatus**	base margaritatus
P. robustus LO	**base margaritatus**						base ibex	davoei	davoei		top ibex	**base margaritatus**	top ibex
L. barozii	**mid davoei**		not studied	top davoei (6)			tenuicostatum	base margaritatus	base margaritatus' / top margaritatus"		mid emaciatum	**top davoei**	
B. grande	mid ibex						mid spinatum	mid stokesi	base margaritatus" / stokesi'	not studied	stokesi /margaritatus	base margaritatus	
S. cruciulus	**base jamesoni**				**mid jamesoni**	**very base jamesoni (7)**	**mid jamesoni**	base jamesoni	mid jamesoni	mid jamesoni	**base jamesoni**	unzoned just earlier jamesoni	top raricostatum
M. protensa	top raricostatum						very base jamesoni		not studied			very base raricostatum	
M. lenticularis	**base raricostatum**						mid raricostatum	top raricostatum	not studied		very base raricostatum	earlier than raricostatum	

In bold are shown consistent events. (1) in Mattioli et al. (2013) this event occurs in an undated interval between Margaritatus and Emaciatum zones; (2) in Mattioli et al. (2013) this event occurs at the top Emaciatum Zone, in which the FCO of *L. sigillatus* occurs; (3) as stated by Mattioli and Erba (1999), *E. britannica* of Hamilton (1977, 1979) are very likely thick *L. frodoi*, which are common in Peniche at the base of the Toarcian (Mailliot et al., 2007); (4) the basal part of the upper Sinemurian only outcrops in Quarries 1 and 2 which were not studied by Hamilton (1977; see Fig. 1). The Sinemurian in Brenha belongs to the Coimbra Fm that does not contain ammonites and is made of hard limestone. The layers where Hamilton (1977) took the samples where *Z. erectus* is reported belong to the lower Pliensbachian Vales das Fontes Fm. Our data show that *Z. erectus* is rare in Brenha whereas *P. liasicus* is common. Hence the common *Z. erectus* reported by Hamilton (1977) likely correspond to misinterpreted *P. liasicus*; (5) *Striatomarginis primitivus* and *Palaeopontosphaera veterna* from Hamilton (1979; pictures 17 and 18) should be ascribed to *L. sigillatus*. Hamilton (1979 stated: "This group includes very small specimens of the genus *Ellipsagelosphaera* which cannot be identified at species level because of their small size. These specimens may be the ancestral forms of *Ellipsagelosphaera britannica*"; (6) the FO of *Lotharingius* spp. reported by Bergen in Portugal likely corresponds to *L. barozii*; (7) *S. orbiculus*. We consider the small *Similiscutum* all together; (8) Aguado et al. (2008) states that *W. britannica* and *W. communis* are present in the uppermost Aalenian; (9) calcareous nannofossil data in Peti et al. (2015) come from Boulila et al. (2014); (10) pictures of this species are lacking in Peti et al. (2017). However, the anomalous early record of *L. crucicentralis* might be due to presence of misidentified specimens of *L. sigillatus* in the Margaritatus Zone; (11) according to the pictures shown, it corresponds to *L. frodoi*.

literature are herein equivalent to its FCO (late Pliensbachian Emaciatum Zone).

Discrepancies also occur for the FO of *Watznaueria britannica* which was previously deemed a good marker for the Aalenian/Bajocian boundary (Mattioli and Erba, 1999). After a thorough review, the FO of *W. britannica* morphotypes A, B and D are herein recorded in the middle part of the Murchisonae Zone (middle Aalenian), whereas morphotypes E, F and C first occur in the upper part of Concavum Zone. *Watznaueria britannica* morphotypes A and B correspond to relatively small coccoliths, whereas morphotype C is characterized by large specimens with a relatively wide central area spanned by a thin bar (Giraud et al., 2006). This study shows for the first time the FO of the various morphotypes of *W. britannica*, as Giraud et al. (2006) only dealt with Oxfordian material. The anomalous record of *Ellipsagellosphaera* (syn. *Watznaueria*) *britannica* reported in the basal Toarcian by Hamilton (1979) in Portuguese sections is most likely due to the presence of overgrown specimens of large *L. frodoi* (Plate 1). Mailliot et al. (2007) observed in various lower Toarcian samples from the Peniche section, overgrown specimens of *L. frodoi* with high birefringence colours and a structure in the central area mimicking a transverse bridge. These specimens probably correspond to transitional forms between *Lotharingius* and *Watznaueria britannica* morphotype F as described by Giraud et al.

(2006). The Aalenian has received relatively less attention than the Toarcian age, and nannofossil biostratigraphy can be more complex during this time interval due to the coexistence of *Watznaueria* species with a cross structure in the central area (*W. colacicchii*, *W. contracta*, *W.* aff. *W. contracta*) and with a transversal bar, such as *W. britannica* morphotypes.

6.1.3. Discrepancies due to sedimentary features

The late Pliensbachian and the early Toarcian are intervals where important glacio-eustatic sea level changes occurred (Guex et al., 2001; Pittet et al., 2014). Condensations and hiatuses happened both related to sea level low and to subsequent fast transgressions (Pittet et al., 2014). Such sedimentary features greatly affected the nannofossil record, particularly at the Pliensbachian/Toarcian transition and in the ensuing Polymorphum Zone. This can be at the origin for the discrepancies observed in the record of the FO of *L. crucicentralis* (Table 1), but also for *D. ignotus* and *C. superbus*. In fact, the latter two species occur in the Polymorphum Zone during the Pliensbachian/Toarcian negative $\delta^{13}C$ excursion and subsequent positive $\delta^{13}C$ rebound. However, two important, supra-regional discontinuities occurred at that time: a condensation and a hiatus (D1 and D2 in Pittet et al., 2014). During the subsequent T-OAE negative $\delta^{13}C$ excursion, nannofossils

experienced a dramatic decrease in abundance that culminated with their blackout in some regions (Bucefalo Palliani et al., 2002; Mattioli et al., 2009). *Discorhabdus ignotus* in particular, acts like a Lazarus species during the T-OAE, re-emerging with a consistent record in the aftermath of the isotopic perturbation (Mattioli et al., 2013; FCO in Fig. 2). Nannofossil biostratigraphy is therefore quite complex in the interval comprised between the Pliensbachian/Toarcian boundary and the end of the T-OAE, but due to their remarkable continuity, the Portuguese sections represent an excellent record of this time inteval and allow a better understanding of the succession of nannofossil events.

6.2. New nannofossil zonation for the Lusitanian Basin

Between the late Sinemurian and the early Bajocian, Portuguese sections yielded almost 100 nannofossil bioevents (Fig. 2) comprising not only the index species FO and LO but also, when suitable, their FCO, LCO, RI and RD. A common pattern in nannofossil distribution seems to be the discontinuous record of a given taxon after its FO is observed, and then followed by its consistent record. Hence, in certain cases also RI and RD may bear biostratigraphic information. This is the first time such an approach is used with Jurassic nannofossils, although a similar approach has already been successfully used for the Paleogene stratigraphy by Agnini et al. (2014). In order to improve the biochronological resolution of nannofossil zonation with regard to feature schemes (Bown and Cooper, 1998; Mattioli and Erba, 1999), 28 bioevents are used herein to define nannofossil zones and subzones (Fig. 3). In order to avoid major divergences with the literature, zonal markers used in previous schemes are whenever possible kept. The NJT6 Zone (*Carinolithus superbus*) for example, is widely used in the literature as it comprises the δ^{13}C negative excursion of the T-OAE. Consequently, all of the zone defining criteria are preserved with regard to Bown and Cooper (1998) and Mattioli and Erba (1999). However, the chronostratigraphic duration of the new zones is in most cases different with respect to the literature, as some index species (e.g., *Retecapsa incompta*) turn out to appear much earlier than what had been previously reported. Nonetheless, in order to obtain a stratigraphic resolution as high as ammonite biostratigraphy, a relatively high number of subzones are here introduced. In some cases, these subzones are defined in order to constrain as closely as possible marked δ^{13}C and δ^{18}O excursions which in turn correspond to important palaeoceanographic or palaeoclimatic events.

6.3. Nannofossil evolution and δ^{13}C and δ^{18}O excursions

Between the Sinemurian and Bajocian ages, major δ^{13}C and δ^{18}O events are acknowledged in the Lusitanian Basin (Fig. 4) and are as of now, dated by a comprehensive nannofossil zonation scheme. Some of these isotopic events match important steps in the early evolution of Jurassic coccolithophores. The Sinemurian/Pliensbachian δ^{13}C negative excursion already recorded by Duarte et al. (2014) from bulk rock samples is corroborated by our new data obtained from brachiopod calcite (Fig. 4). In fact, the sharp negative shift of δ^{13}C values observed within the late Sinemurian (Raricostatum Zone) suggests that this excursion started before the Sinemurian/Pliensbachian boundary at the basal NJT3c Subzone. During that time interval, the tiered placolith genus *Mazaganella* and the radiating placoliths of the genus *Similiscutum* arose. The entry of new Biscutaceae placolith-coccoliths makes the early Pliensbachian one of the most important time intervals in coccolithophore evolution. Actually, the emergence of the placolith morphology allow coccoliths to physically inter-lock and form for the first time a coccosphere able to fossilize. Prior to this morphological innovation, the murolith-coccoliths were presumably bound together around the cell by organic material (Bown, 1987) and once the coccospheres were buried within sediments, they would then crumble. Although it is unclear how the placolith morphology did appear in

western Tethys and from which ancestor it evolved from (Bown, 1987), it cannot be excluded that following the opening of the Hispanic Corridor during the earliest Pliensbachian, these coccoliths might have migrated from the Panthalassa Ocean (Plancq et al., 2016; Wiggan et al., 2018). A similar explanation is provided by van de Schootbrugge et al. (2005) to explain the invasion of the Tethys by the palaeo-Pacific dinoflagellate *Liasidium variabile*.

The second phase in placolith evolution is characterized by the introduction of more complex imbricated coccoliths with a bicyclic distal shield. The FO of *Lotharingius barozii* in the uppermost part of the early Pliensbachian illustrates this evolutionary step, as it probably evolved from the bicyclic radiating placolith *Bussonius*. This phase corresponds to the Davoei Zone thermal peak (Silva et al., 2011; Silva and Duarte, 2015) at the NJT4b/NJT4c boundary. Throughout the ensuing Margaritatus Zone, the low brachiopod δ^{18}O values suggest an episode of warm bottom water temperatures during which several species of the *Lotharingius* genus first appeared. During an episode of extreme cooling in the Emaciatum (Spinatum) Zone, as indicated by a marked increase in oxygen isotope values suggesting that bottom water temperatures drop by ~7 °C with regard to the previous Margaritatus Zone (Suan et al., 2008, 2010), small forms of *Biscutum* (*B. dubium* and *B. intermedium*) and two *Lotharingius* species that will later dominate the coccolithophore community (L. *crucicentralis* and *L.* velatus), emerge. NJT5b Subzone spans across almost the totality of this event and again, data show that extreme environmental changes are likely connected to the appearance of new species. The extensively studied Pliensbachian/Toarcian δ^{13}C negative excursion (e.g., Hesselbo et al., 2007; Suan et al., 2008, 2010; Pittet et al., 2014) matches the base of the NJT5c Subzone, when the first species of the *Zeugrhabdotus* genus occurs. Coeval with a severe cooling and likely the onset of a glacio-eustatic sea level low (Guex et al., 2001; Pittet et al., 2014), NJT5b and NJT5c Subzones correspond to a period of probable allopatric speciation of placolith-coccoliths (Menini et al., 2019). From this moment on, placoliths replace the murolith morphology in terms of abundance and dominate the coccolith floras for the remainder of the Jurassic (Bown, 1987; Mattioli and Erba, 1999; Menini et al., 2019). The widely-studied T-OAE interval occurs "shortly" after the arrival of the *Carinolithus* genus and the ensuing Levisoni warming period as shown by δ^{18}O excursions (Suan et al., 2008, 2010; Ferreira et al., 2015), spanning throughout almost the entire NJT6 Zone. Values in δ^{13}C reach their maxima within this zone, increasing by a staggering ~3.0‰ before dropping, hence unambiguously describing a positive excursion throughout part of NJT6 and the Levisoni Zone (see also Duarte et al., 2007 and Hesselbo et al., 2007 for bulk carbonate samples). In the aftermath of the T-OAE and during the Levisoni δ^{13}C positive excursion, the FCO of small *Discorhabdus ignotus* is observed and only *Mitrolithus jansae* becomes extinct. During the rebuilding of marine ecosystems that followed the T-OAE, the genus *Watznaueria* is recorded for the first time ever. The FO of *W. fossacincta* and later of its siblings, is quite significant as this genus will numerically dominate the nannofossil assemblages for the remaining Mesozoic. From the Bifrons and NJT7 Zone, δ^{13}C values start returning to their pre-excursion record while a steady and long-term increase in δ^{18}O values commences. During this interval, a significant increase in the mean size of all the *Lotharingius* species occur (Ferreira et al., 2017). Such size shift is partly related to a species-specific replacement within the *Lotharingius* pool, where abundant early Toarcian small-sized species are replaced by large-sized ones during the middle and late Toarcian. This pattern however, was also accompanied by the size increase of all *Lotharingius* morphospecies across the middle Toarcian.

Bottom water temperatures reached their minima within NJT8f Subzone when a drastic cooling of ~6 °C is suggested by brachiopod oxygen isotope values near the Toarcian-Aalenian transition, and across the Opalinum Zone (Fig. 4). No new taxa occur during this period and a sharp, distinctive decrease in *Lotharingius crucicentralis* relative abundance is recorded. After this extreme cooling event, and still within a

steady long-term temperature decline interval, the radiation of *Watznaueria* accelerated from the middle Aalenian up to the early Bajocian. During ~2 Myr, from NJT8g to NJT9d Subzones, new *Watznaueria* morphotypes occurred: with a cross in their central area (*W.* aff. *W. contracta*), with a bar in their central area (*W. britannica* types A, B, D, and *W. communis*) and ultimately, with a closed central area (*W.* aff. *W. manivitiae*). Although already suggested by Jenkyns et al. (2002) and supported by the bulk carbonate data by Suchéras-Marx et al. (2012) in the Cabo Mondego section, the Discites δ^{13}C negative excursion is not clearly perceivable in brachiopod calcite likely due to the low sampling density in this interval. However, a decrease in δ^{13}C values is observed from the NJT9 Zone coeval with the *Watznaueria* speciation. This radiation reflects the decrease in abundance of *Lotharingius* species already observed in other works (e.g., Ferreira et al., 2015; Giraud et al., 2016; Aguado et al., 2017; Wiggan et al., 2018), particularly that of L. *crucicentralis* whose RD happens at the temperature minimum, and of L. *velatus*. The *Watznaueria* radiation and its subsequent ecological dominance was not made at the expenses of other genera but through its integration in the coccolithophore community (Suchéras-Marx et al., 2015). The expansion of *Watznaueria* occurred in two separate steps: first, during the latest Aalenian and earliest Bajocian, where morphotypes with a cross in their central area such as *W. colacicchii, W. contracta* and *W.* aff. *W. contracta* dominated (Suchéras-Marx et al., 2015; Giraud et al., 2016; Wiggan et al., 2018); and second, during the early Bajocian when species lacking a central cross, those with a central bar and those with a closed central area such as *W.* aff. *W. manivitiae* and *W. manivitiae* increased their abundance (Giraud et al., 2016). The *Watznaueria* upsurge roughly coincides with the Propinquans positive excursion, when δ^{13}C values steadily and consistently increase by ~1‰. This phase of increased surface water fertility starts from the early Bajocian and defines the base of the NJT10 Zone.

7. Conclusions

This account presents a unique, thorough and systematic nannofossil analysis of ~800 m thick west Tethyan successions spanning ~24 Myr and yieldeding a comprehensive biostratigraphic scheme for the Early and Middle Jurassic epochs. Nearly 100 biostratigraphic horizons (FO, LO, FCO, LCO, RI and RD) have been identified through repeated sample double-check and taxa blind test assessment. This endeavour tries to reconcile two major zonation schemes widely used in the literature for two discrete Tethyan provinces and thus, nannofossil zones previously defined for NW Europe and Mediterranean provinces are kept. The significant number of subzones recognized - 30 subzones - allows a more detailed chronostratigraphic resolution for the Early and Middle Jurassic interval. In fact, the average duration of the newly defined nannofossil zones is 2.7 Myr (from ~1.5 Myr in NJT6 to ~6 Myr in NJT8), while the average duration for subzones is 0.8 Myr (from ~0.1 Myr in NJT9d to 1.6 Myr in NJT4c). Although bearing different evolutionary patterns, the nannofossil subzones defined herein, have a time resolution close to, or higher than, that of ammonites. More importantly, in this new zonation scheme, all major stage or substage boundaries are defined with respect to a precise nannofossil zone or subzone: 1) the Sinemurian/Pliensbachian boundary in NJT3c; 2) the early/late Pliensbachian in NJT4c; 3) the Pliensbachian/Toarcian boundary that also corresponds to the GSSP at Peniche, dated at 182.7 Ma, matches the NJ5b/NJT5c boundary; 4) the early/middle Toarcian in NJT7a; 5) the middle/late Toarcian in NJT8b; 6) the Toarcian/Aalenian (Early/Middle Jurassic) in NJT8d; 7) the early/middle Aalenian in the upper part NJT8f; 8) the middle/late Aalenian defined by the base of NJT9b; 9) the Aalenian/Bajocian boundary also representing the GSSP at Cabo Mondego, dated at 170.3 Ma, corresponds to the base of NJT9c.

For the first time, all the major C and O isotope excursions recorded in this time interval by brachiopod shells and marking major palaeoclimatic and palaeoceanographic events are here dated by means of

nannofossil zones: the Sinemurian/Pliensbachian δ^{13}C negative excursion in NJT3c; the Davoei event at the NJT4b/NJT4c boundary; the Emaciatum cooling event in NJT5b; the Pliensbachian/Toarcian δ^{13}C negative excursion at the NJT5b/NJT5c boundary; the T-OAE negative excursion in NJT6a; the Levisoni δ^{13}C positive excursion in NJT6b; the Opalinum extreme cooling event in NJT8f and the Propinquans δ^{13}C positive excursion in NJT10a.

The sometimes scarce and discontinuous ammonite record and their characteristic palaeoprovincialism during the Early and Middle Jurassic epochs can, from this work, be surpassed since the occasionally ambiguous ammonite zones boundaries can now be correlated to chemo and nannofossil biostratigraphy. This work also demonstrates that the continuous and contiguous record of calcareous nannofossil allows to attain a high-resolution (interval zones) scheme for the Early and Middle Jurassic, thus showing the relevance of these organisms as performant biochronological tools.

Appendix A. Supplementary data

Supplementary data to this article can be found online at https://doi.org/10.1016/j.earscirev.2019.102908.

References

Agnini, C., Fornaciari, E., Raffi, I., Catanzariti, R., Pälike, H., Backman, J., Rio, D., 2014. Biozonation and biochronology of Paleogene calcareous nannofossils from low and middle latitudes. Newsl. Stratigr. 47 (2), 131–181.

Aguado, R., O'Dogherty, L., Sandoval, J., 2008. Fertility changes in surface waters during the Aalenian (mid-Jurassic) of the western Tethys as revealed by calcareous nannofossils and carbon-cycle perturbations. Mar. Micropaleontol. 68, 268–285.

Aguado, R., O'Dogherty, L., Sandoval, J., 2017. Calcareous nannofossil assemblage turnover in response to the early Bajocian (middle Jurassic) palaeoenvironmental changes in the Subbetic Basin. Palaeogeogr. Palaeoclimatol. Palaeoecol. 472, 128–145.

Alves, T.M., Gawthorpe, R.L., Hunt, D.W., Monteiro, J.H., 2002. Jurassic tectono-sedimentary evolution of the Northern Lusitanian Basin (offshore Portugal). Mar. Pet. Geol. 19, 727–754.

Arias, C., 2007. Pliensbachian-Toarcian ostracod biogeography in NW Europe: evidence for water mass structure evolution. Palaeogeogr. Palaeoclimatol. Palaeoecol. 251, 398–421.

Auclair, A.-C., Joachimski, M.M., Lécuyer, C., 2003. Deciphering kinetic, metabolic and environmental controls on stable isotope fractionations between seawater and shell of Tetrabratalia transversa (Brachiopoda). Chem. Geol. 202, 59–78.

Azerêdo, A.C., Duarte, L.V., Henriques, M.H., Manuppella, G., 2003. Da dinâmica continental no Triásico aos mares do Jurássico Inferior e Médio. Cadernos de Geologia de Portugal. Instituto Geológico e Mineiro, Lisboa, pp. 43.

Azerêdo, A.C., Duarte, L.V., Silva, R.L., 2014. Configuração sequencial em ciclos (2 ordem) de fácies transgressivas-regressivas do Jurássico Inferior e Médio da Bacia Lusitâinca (Portugal). Comunicacões Geológicas 101, 383–386 Especial I.

Bassoulet, J.P., Elmi, S., Poisson, A., Cecca, F., Bellion, Y., Guiraud, R., Baudin, F., 1993. Mid Toarcian. In: Dercourt, J., Ricou, L.E., Vrielynck, B. (Eds.), Atlas of Tethys Paleoenvironmental Maps. Becip-Franlab, Rueil-Malmaison, France, pp. 63–80.

Bjerrum, C.J., Surlyk, F., Callomon, J.H., Slingerland, R.L., 2001. Numerical Paleoceanographic study of the early Jurassic transcontinental Laurasian Seaway. Paleoceanography 16, 390–404.

Bown, P.R., 1987. Taxonomy, evolution and biostratigraphy of Late Triassic-Early Jurassic calcareous nannofossils. Spec. Pap. Palaeontol. 38, 1–118.

Bown, P.R., Cooper, M.K.E., 1989. New calcareous nannofossil taxa from the Jurassic. J. Micropalaeontol. 8, 91–96.

Bown, P.R., Cooper, M.K.E., 1998. Jurassic. In: Bown, P.R. (Ed.), Calcareous Nannofossils Biostratigraphy. British Micropalaeontological Society Publication Series, Kluver Academic Publishers, Cambridge, pp. 34–85.

Bown, P.R. with contributions from the International Nannoplankton Association, Jurassic Working Group, 1996. Recent advances in Jurassic calcareous nannofossil research. GeoResearch Forum 1-2, 55–66.

Bown, P.R., Cooper, M.K.E., Lord, A.R., 1988. A calcareous nannofossil Biozonation scheme for the early to mid Mesozoic. Newslett. Stratigr. 20, 91–111.

Brand, U., Azmy, K., Bitner, M.A., Logan, A., Zuschin, M., Came, R., Ruggiero, E., 2014. Oxygen isotopes and MgCO₃ in brachiopod calcite and a new paleotemperature equation. Chem. Geol. 359, 23–31.

Bucefalo Palliani, R., Riding, J.B., 2003. Biostratigraphy, provincialism and evolution of European Early Jurassic (Pliensbachian to Early Toarcian) dinoflagellate cysts. Palynology 27, 179–214.

Bucefalo Palliani, R., Mattioli, E., Riding, J.B., 2002. The response of marine phytoplankton and sedimentary organic matter to the early Toarcian (Lower Jurassic) oceanic anoxic event in northern England. Mar. Micropaleontol. 46, 223–245.

Carpenter, S.J., Lohmann, K.C., 1995. ¹⁸O and ¹³C values of modern brachiopod shells. Geochim. Cosmochim. Acta 59, 3749–3764.

Cobianchi, M.A., 1992. Sinemurian-Early Bajocian Calcareous Nannofossil Biostratigraphy of the Lombardy Basin (Southern Calcareous Alps; Northern Italy). Atti Ticinensi Sc. Terra 35, 61–106.

Comas-Rengifo, M.J., Duarte, L.V., Goy, A., Paredes, R., Silva, R.L., 2013. El Sinemuriense Superior (cronozonas Oxynotum y Raricostatum) en la región de S. Pedro de Moel (Cuenca Lusitánica, Portugal). Comunicações Geológicas 100, 15–19 Especial I.

Copestake, P., Johnson, B., 2014. Lower Jurassic Foraminifera from the Llandbedr (Mochras Farm) Borehole, North Wales, UK. Monograph of The Paleontographical Society, London, pp. 403.

Cresta, S., Goy, A., Ureta, S., Arias, C., Barrón, E., Bernard, J., Canales, M.L., García-Joral, F., García- Romero, E., Gialanella, P.R., Gómez, J.J., González, J.A., Herrero, C., Martínez, G., Osete, M.L., Perilli, N., Villalaín, J.J., 2001. The global stratotype section and point (GSSP) of the Toarcian-Aalenian boundary (Lower-Middle Jurassic). Episodes 24, 166–175.

de Kaenel, E., Bergen, J.A., 1993. New early and middle Jurassic coccolith taxa and biostratigraphy from the eastern proto-Atlantic (Morocco, Portugal and DSDP Site 547B). Eclogae Geol. Helv. 86, 861–908.

de Kaenel, E., Bergen, J.A., von Salis Perch-Nielsen, K., 1996. Jurassic calcareous nannofossil biostratigraphy of western Europe. Compilation of recent studies and calibration of bioevents. Bulletin de la Societe Géologique de France 167, 15–28.

Deflandre, G., Fert, C., 1954. Observations sur les coccolithophoridés actuels et fossiles en microscopie ordinaire et électronique. Ann/s. Paléont 40, 115–176.

Dera, G., Brigaud, B., Monna, F., Laffont, R., Pucéat, E., Deconinck, J.-F., Pellenard, P., Joachimski, M.M., Durlet, C., 2011a. Climatic ups and downs in a disturbed Jurassic world. Geology 39, 215–218.

Dera, G., Neige, P., Dommergues, J.-L., Brayard, A., 2011b. Ammonite paleobiogeography during the Pliensbachian-Toarcian crisis (Early Jurassic) reflecting paleoclimate, eustasy, and extinctions. Glob. Planet. Chang. 78, 92–105.

Dercourt, J., Gaetani, M., Vrielynck, B., Barrier, E., Biju Duval, B., Brunet, M.F., Cadet, J.P., Crasquin, S., Sandulescu, M., 2000. Atlas Peri-Tethys, Palaeogeographical Maps. CCGM/CGMW, Paris.

Dommergues, J.L., Fara, E., Meister, C., 2009. Ammonite diversity and its palaeobiogeographical structure during the early Pliensbachian (Jurassic) in the western Tethys and adjacent areas. Palaeogeogr. Palaeoclimatol. Palaeoecol. 280, 64–77.

Duarte, L.V., 1997. Facies analysis and sequential evolution of the Toarcian-Lower Aalenian series in the Lusitanian Basin (Portugal). Comunicações do Instituto Geológico e Mineiro 83, 65–94.

Duarte, L.V., 2007. Lithostratigraphy, sequence stratigraphy and depositional setting of the Pliensbachian and Toarcian series in the Lusitanian Basin (Portugal). In: Rocha, R.B. (Ed.), The Peniche Section (Portugal). Contributions to the Definition of the Toarcian GSSP. International Subcommission on Jurassic Stratigraphy, pp. 17–23.

Duarte, L.V., Soares, A.F., 2002. Litostratigrafia das séries margo-calcárias do Jurássico inferior da Bacia Lusitânica (Portugal). vol. 89. Comunicações do Instituto Geológico e Mineiro, pp. 135–154.

Duarte, L.V., Oliveira, L.C., Rodrigues, R., 2007. Carbon isotopes as a sequence stratigraphic tool: examples from the lower and Middle Toarcian marly limestones of Portugal. Bol. Geol. Min. 118, 3–17.

Duarte, L.V., Silva, R.L., Oliveira, L.C.V., Comas-Rengifo, M.J., Silva, F., 2010. Organic-rich facies in the Sinemurian and Pliensbachian of the Lusitanian Basin, Portugal: Total Organic Carbon and relation to transgressive-regressive facies cycles. Geol. Acta 8, 325–340.

Duarte, L.V., Silva, R.L., Mendonça Filho, J.G., Poças Ribeiro, N., Chagas, R.B.A., 2012. High-resolution stratigraphy, palynofacies and source rock potential of the Água de Madeiros Formation (Lower Jurassic), Lusitanian Basin, Portugal. J. Pet. Geol. 35, 105–126.

Duarte, L.V., Comas-Rengifo, M.J., Silva, R.L., Paredes, R., Goy, A., 2014. Carbon isotope stratigraphy and ammonite biochronostratigraphy across the Sinemurian-Pliensbachian boundary in the western Iberian margin. Bull. Geosci. 89 (4), 719–736.

Fatela, F., Taborda, R., 2002. Confidence limits of species proportions in microfossil assemblages. Mar. Micropaleontol. 45, 169–174.

Ferreira, J., Mattioli, E., Pittet, B., Cachão, M., Spangenberg, J.E., 2015. Palaeoecological insights on Toarcian and lower Aalenian calcareous nannofossils from the Lusitanian Basin (Portugal). Palaeogeogr. Palaeoclimatol. Palaeoecol. 436, 245–262.

Ferreira, J., Mattioli, E., van de Schootbrugge, B., 2017. Palaeoenvironmental *vs.* evolutionary control on size variation of coccoliths across the Lower-Middle Jurassic. Palaeogeogr. Palaeoclimatol. Palaeoecol. 465, 177–192.

Fraguas, A., Erba, E., 2010. Biometric analyses as a tool for the differentiation of two coccolith species of the genus Crepidolithus (Pliensbachian, Lower Jurassic) in the Basque-Cantabrian Basin (Northern Spain). Mar. Micropaleontol. 77, 125–136.

Fraguas, A., Young, J., 2011. Evolution of the coccolith genus *Lotharingius* during the Late Pliensbachian-Early Toarcian interval in Asturias (N Spain). Consequences of the Early Toarcian environmental perturbations. Geobios 44, 361–375.

Fraguas, A., Comas-Rengifo, M.J., Perilli, N., 2015. Calcareous nannofossil biostratigraphy of the Lower Jurassic in the Cantabrian Range (Northern Spain). Newsl. Stratigr. 48 (2), 179–199.

Fraguas, A., Comas-Rengifo, Goy, Gómez, J.J., 2018. Upper Sinemurian-Pliensbachian calcareous nannofossil biostratigraphy of the E Rodiles section (Asturias, N Spain): a reference section for the connection between the Boreal and Tethyan Realms. Newslett. Stratigr. 51 (2), 227–244.

Geisen, M., Bollman, J., Herrle, J.O., Mutterlose, J., Young, J.R., 1999. Calibration of the random settling technique for calculation of absolute abundances of calcareous nannoplankton. Micropaleontology 45, 437–442.

Giraud, F., Pittet, B., Mattioli, E., Audouin, V., 2006. Paleoenvironmental controls on morphology and abundance of the coccolith *Watznaueria britannica* (Late Jurassic, southern Germany). Mar. Micropaleontol. 60, 205–225.

Giraud, F., Mattioli, E., López-Otálvaro, G.E., Lécuyer, C., Suchéras-Marx, B., Alméras, Y., Martineau, F., Arnaud-Godet, F., de Kænel, E., 2016. Deciphering processes controlling mid-Jurassic coccolith turnover. Mar. Micropaleontol. 125, 36–50.

Goy, G., 1981. Nannofossiles calcaires des schistes carton (Toarcien Inferieur) du Bassin de Paris. Doc. de la RCP 459, Nature et genèse des facies confinés. (Editions du BRGM 1-86).

Gradstein, F.M., Ogg, J.G., Schmitz, M., Ogg, G., 2012. The Geological Time Scale 2012. Elsevier.

Guex, J., Morard, A., Bartolini, A., Morettini, E., 2001. Découverte d'une importante lacune stratigraphique à la limite Domérien-Toarcien: implications paléoocéanographiques. Bulletin de la Société Vaudoise des. Sciences Naturelles 345, 277–284.

Hamilton, G., 1977. Early Jurassic calcareous nannofossils from Portugal and their biostratigraphic use. Eclogae Geol. Helv. 72, 575–598.

Hamilton, G., 1979. Lower and Middle Jurassic calcareous nannofossils from Portugal. Eclogae Geol. Helv. 72, 1–17.

Henriques, M.H., Canales, M.L., Silva, S.C., Figueiredo, V., 2016. Integrated biostratigraphy (Ammonoidea, Foraminiferida) of the Aalenian of the Lusitanian Basin (Portugal): a synthesis. Episodes 39, 482–490.

Hesselbo, S.P., Jenkyns, H.C., Duarte, L.V., Oliveira, L.C.V., 2007. Carbon-isotope record of the Early Jurassic (Toarcian) Oceanic Anoxic Event from fossil wood and marine carbonate (Lusitanian Basin, Portugal). Earth Planet. Sci. Lett. 253, 455–470.

Ivimey-Cook, H.C., 1971. Stratigraphical palaeontology of the Lower Jurassic of the Llanbedr (Mochras Farm) Borehole. In: Woodland, A.W. (Ed.), The Llanbedr (Mochras Farm) Borehole. Institute of Geological Sciences, pp. 87–92 Report no. 71/18.

Jenkyns, H.C., 1988. The Early Toarcian (Jurassic) anoxic event: stratigraphic, sedimentary and geochemical evidence. Am. J. Sci. 288, 101–151.

Jenkyns, H.C., Jones, C.E., Gröcke, D.R., Hesselbo, S.P., Parkinson, D.N., 2002. Chemostratigraphy of the Jurassic System: applications, limitations and implications for palaeoceanography. J. Geol. Soc. 159, 351–372.

Jones, C.E., Jenkyns, H.C., Coe, A.L., Hesselbo, S.P., 1994. Strontium isotopic variations in Jurassic and cretaceous seawater. Geochim. Cosmochim. Acta 58, 3061–3074.

Jourdan, F., Féraud, G., Bertrand, H., Watkeys, M.K., Renne, P.R., 2007. Distinct brief major events in the Karoo large igneous province clarified by new ⁴⁰Ar/³⁹Ar ages on the Lesotho basalts. Lithos 98, 195–209.

Kullberg, J.C., Rocha, R.B., Soares, A.F., Rey, J., Terrinha, P., Azerêdo, A.C., Callapez, P., Duarte, L.V., Kullberg, M.C., Martins, L., Miranda, J.R., Alves, C., Mata, J., Madeira, J., Mateus, O., Moreira, M., Nogueira, C.R., 2013. A Bacia Lusitaniana: estratigrafia, paleogeografia e tectónica. Geologia de Portugal 2, 195–347.

López-Otálvaro, G.-E., Henriques, M.H., 2018. High-resolution calcareous nannofossil biostratigraphy from the Bathonian ASSP of the Cabo Mondego Section (Lusitanian Basin, Portugal). Newsl. Stratigr. https://doi.org/10.1127/nos/2018/0452.

López-Otálvaro, G.-E., Baptiste Suchéras-Marx, B., Giraud, F., Mattioli, E., Lécuyer, C., 2012. *Discorhabdus* as a key coccolith genus for paleoenvironmental reconstructions (Middle Jurassic, Lusitanian Basin): Biometry and taxonomic status. Mar. Micropaleontol. 94-95, 45–57.

Lozar, F., 1992. Biostratigrafia a Nannofossili calcarei nel Lias: risultati di alcune sezioni nel Bacino Lombardo e nel Bacino Delfinese. Paleopelagos 2, 89–98.

Lozar, F., 1995. Calcareous nannofossil biostratigraphy of lower Liassic from Western Tethys. Palaeontographia Italica 82, 91–121.

Macchioni, F., 2002. Myths and legends in the correlation between the Boreal and Tethyan Realms. Implications on the dating of the Early Toarcian mass extinctions and the Oceanic Anoxic Event. Geobios 35 (M.S. 24), 150–164.

Macchioni, F., Cecca, F., 2002. Biodiversity and biogeography of middle-late iassic ammonoids: implications for the Early Toarcian mass extinction. Geobios 35 (M.S. 24), 165–175.

Mailliot, S., Elmi, S., Mattioli, E., Pittet, B., 2007. Calcareous nannofossil assemblages across the Pliensbachian/Toarcian boundary at the Peniche section (Ponta do Trovão, Lusitanian Basin). Ciências da Terra 15, 1–14.

Mattioli, E., 1996. New calcareous nannofossil species from the early Jurassic of Tethys. Riv. Ital. Paleontol. Stratigr. 102, 397–412.

Mattioli, E., Erba, E., 1999. Biostratigraphic synthesis of calcareous nannofossil events in the Tethyan Jurassic. Riv. Ital. Paleontol. Stratigr. 105, 343–376.

Mattioli, E., Pittet, B., Young, J.R., Bown, P.R., 2004. Biometric analysis of Pliensbachian-Toarcian (Lower Jurassic) coccoliths of the family Biscutaceae: intra- and inter-specific variability versus palaeoenvironmental influence. Mar. Micropalaeontol. 52, 5–27.

Mattioli, E., Pittet, B., Suan, G., Mailliot, S., 2008. Calcareous nannoplankton across the Early Toarcian Anoxic Event: implications for paleoceanography within the western Tethys. Paleoceanography 23, PA3208.

Mattioli, E., Pittet, B., Petitpierre, L., Mailliot, S., 2009. Dramatic decrease of pelagic carbonate production by nannoplankton across the Early Toarcian anoxic event (T-OAE). Glob. Planet. Chang. 65, 134–145.

Mattioli, E., Plancq, J., Boussaha, M., Duarte, L.V., Pittet, B., 2013. Calcareous nannofossil biostratigraphy: new data from the Lower Jurassic of the Lusitanian Basin. Comunicações Geológicas 100, 69–76.

Menini, A., Mattioli, E., Spangenberg, J.E., Pittet, B., Suan, G., 2019. New calcareous nannofossil and carbon isotope data for the Pliensbachian/Toarcian boundary (Early Jurassic) in the western Tethys and their paleoenvironmental implications. Newsl. Stratigr. 52, 173–196.

Mouterde, R., 1955. Le Lias de Peniche. Comunicações dos Serviços Geológicos de Portugal 36, 1–33.

Mouterde, R., Ruget, C., 1975. Esquisse de la paleogeographie du jurassique inférieur et moyen en Portugal. Bull. Soc. Geol. Fr. 14, 779–786.

Noël, D., 1972. Nannofossiles calcaires de sédiments jurassiques finement laminés. Bull. Mus. Nat. Hist. Natur. Paris 75, 95–156.

Noël, D., 1973. Nannofossiles calcaire de sédiments jurassiques finement laminés. Bull. Mus. Nat. Hist. Natur. Paris 75, 95–156.

Parkinson, D., Curry, G.B., Cusack, M., Fallick, A.E., 2005. Shell structure, patterns and trends of oxygen and carbon stable isotopes in modern brachiopod shells. Chem. Geol. 219, 193–235.

Pavia, G., Enay, R., 1997. Definition of the Aalenian-Bajocian Stage boundary. Episodes 20, 16–22.

Perilli, N., 2000. Calibration of early-middle Toarcian nannofossil events based on high-resolution ammonite biostratigraphy in two expanded sections from the Iberian Range (East Spain). Mar. Micropaleontol. 39, 293–308.

Perilli, N., Duarte, L.V., 2006. Toarcian nannobiohorizons from Lusitanian Basin (Portugal) and their calibration against ammonite zones. Riv. Ital. Paleontol. Stratigr. 112, 417–434.

Perilli, N., Goy, A., Comas-Rengifo, M.J., 2004. Calibration of the Pliensbachian-Toarcian calcareous nannofossil zone boundaries based on ammonite (Basque-Cantabrian area, Spain). Riv. Ital. Paleontol. Stratigr. 110, 97–107.

Perilli, N., Fraguas, A., Comas-Rengifo, M.J., 2010. Reproducibility and reliability of the Pliensbachian calcareous nannofossil biohorizons from the Basque-Cantabrian Basin (Northern Spain). Geobios 43, 77–85.

Peti, L., Thibault, N., Clémence, M.-E., Korte, C., Dommergues, J.-L., Bougeault, C., Pellenard, P., Jelby, M.E., Ullmann, C.V., 2017. Sinemurian-Pliensbachian calcareous nannofossil biostratigraphy and organic carbon isotope stratigraphy in the Paris Basin: calibration to the ammonite biozonation of NW Europe. Palaeogeogr. Palaeoclimatol. Palaeoecol. 468, 142–161.

Phelps, R., 1985. A refined ammonite biostratigraphy for the Middle and Upper Carixian (Ibex and Davoei zones, Lower Jurassic) in North-West Europe and stratigraphical details of the Carixian-Domerian boundary. Geobios 18, 321–362.

Pinheiro, L.M., Wilson, R.C.L., Pena dos Reis, R., Whitmarsh, R.B., Ribeiro, A., 1996. The western Iberia margin: A geophysical and geological overview. In: Whitmarsh, R.B., Sawyer, D.S., Klaus, A., Masson, D.G. (Eds.), Proceedings of the Ocean Drilling Program. vol. 149. Scientific Results, pp. 3–23.

Pittet, B., Suan, G., Lenoir, F., Duarte, L.V., Mattioli, E., 2014. Carbon isotope evidence for sedimentary discontinuities in the lower Toarcian of the Lusitanian Basin (Portugal): Sea level change at the onset of the Oceanic Anoxic Event. Sediment. Geol. 303, 1–14.

Plancq, J., Mattioli, E., Pittet, B., Baudin, F., Duarte, L.V., Boussaha, M., Grossi, V., 2016. A calcareous nannofossil and organic geochemical study of marine palaeoenvironmental changes across the Sinemurian/Pliensbachian (early Jurassic, ~191Ma) in Portugal. Palaeogeogr. Palaeoclimatol. Palaeoecol. 449, 1–12.

Price, G.D., 1999. The evidence and implications of polar ice during the Mesozoic. Earth Sci. Rev. 48, 183–210.

Reale, V., Baldanza, A., Monechi, S., Mattioli, E., 1992. Calcareous Nannofossil biostratigraphic events from the Early-Middle Jurassic sequences of the Urnbria-Marche area (Central Italy). Mem. Sc. Geol. Padova. 43, 41–75.

Reggiani, L., Mattioli, E., Pittet, B., Duarte, L.V., Veiga de Oliveira, L.C., Comas-Rengifo, M.J., 2010. Pliensbachian (Early Jurassic) calcareous nannofossils from the Peniche section (Lusitanian Basin, Portugal): a clue for palaeoenvironmental reconstructions. Mar. Micropaleontol. 75, 1–16.

Rocha, R.B., Mattioli, E., Duarte, L.V., Pittet, B., Elmi, S., Mouterde, R., Cabral, M.C., Comas-Rengifo, M.J., Gómez, J.J., Goy, A., Hesselbo, S.P., Jenkyns, H.C., Littler, K., Mailliot, S., Oliveira, L.C.V., Osete, M.L., Perilli, N., Pinto, S., Ruget, C., Suan, G., 2016. Toarcian Stage of Lower Jurassic defined by the Global Boundary Stratotype Section and Point (GSSP) at the Peniche section (Portugal). Episodes 39, 460–481.

Ruban, D.A., Tyszka, J., 2005. Diversity dynamics and mass extinctions of the Early-Middle Jurassic foraminifers: a record from the Northwestern Caucasus. Palaeogeogr.

Palaeoclimatol. Palaeoecol. 222, 329–343.

Sabatino, N., Neri, R., Bellanca, A., Jenkyns, H., Baudin, F., Parisi, G., Masetti, D., 2009. Carbon-isotope records of the Early Jurassic (Toarcian) oceanic anoxic event from the Valdorbia (Umbria–Marche Apennines) and Monte Mangart (Julian Alps) sections: palaeoceanographic and stratigraphic implications. Sedimentology 56, 1307–1328.

Sandoval, J., Bill, M., Aguado, R., O'Dogherty, L., Rivas, P., Morard, A., Guex, J., 2012. The Toarcian in the Subbetic basin (southern Spain): Bio-events (ammonite and calcareous nannofossils) and carbon-isotope stratigraphy. Palaeogeography, Palaeoclimatology. Palaeoecology 342-343, 40–63.

Sandoval, J., 2008. Aalenian carbon isotope-stratigraphy: Calibration with ammonite, radiolarian and nannofossils events in the Western Tethys. Palaeogeography, Palaeoclimatology, Palaeoecology 267, 115–137.

Silva, R.L., Duarte, L.V., 2015. Organic matter production and preservation in the Lusitanian Basin (Portugal) and Pliensbachian climatic hot snaps. Glob. Planet. Chang. 131, 24–34.

Silva, R.L., Duarte, L.V., Comas-Rengifo, M.J., Mendonça Filho, J.G., Azerêdo, A.C., 2011. Update of the carbon and oxygen isotopic records of the Early–Late Pliensbachian (Early Jurassic, ~187 Ma): insights from the organic-rich hemipelagic series of the Lusitanian Basin (Portugal). Chem. Geol. 283, 177–184.

Silva, R.L., Duarte, L.V., Comas-Rengifo, M.J., 2015a. Carbon isotope chemostratigraphy of Lower Jurassic carbonate deposits, Lusitanian Basin (Portugal): Implications and limitations to the application in sequence stratigraphic studies. In: Ramkumar, M. (Ed.), Chemostratigraphy: Concepts, Techniques, and Applications. Elsevier, pp. 341–371.

Silva, S., Henriques, M.H., Canales, M.L., 2015b. High resolution ammonite-benthic foraminiferal biostratigraphy across the Aalenian-Bajocian boundary in the Lusitanian Basin (Portugal). Geol. J. 50, 477–496.

Steinmetz, J.C., 1994. Sedimentation of coccolithophores. In: Winter, A., Siesser, W.G. (Eds.), Coccolithophores. Cambridge University Press, pp. 179–198.

Stradner, H., 1961. Vorkommen von Nannofossilien im Mesozoikum und Alttertiär. Erdoel-Zeitschrift 77, 77–88.

Stradner, H., 1963. New contributions to Mesozoic stratigraphy by means of nannofossils. In: Proc. 6th World Petra. Congr., pp. 167–184 Section 1, Paper 4 (preprint).

Suan, G., Mattioli, E., Pittet, B., Mailliot, S., Lécuyer, C., 2008. Evidence for major environmental perturbation prior to and during the Toarcian (Early Jurassic) oceanic anoxic event from the Lusitanian Basin, Portugal. Paleoceanography 23, PA1202.

Suan, G., Mattioli, E., Pittet, B., Lécuyer, C., Suchéras-Marx, B., Duarte, L.V., Philippe, M., Reggiani, L., Martineau, F., 2010. Secular environmental precursors to early Toarcian (Jurassic) extreme climate changes. Earth Planet. Sci. Lett. 290, 448–458.

Suchéras-Marx, B., Mattioli, E., Pittet, B., Escarguel, G., Suan, G., 2010. Astronomically-paced coccolith size variations during the early Pliensbachian (Early Jurassic). Palaeogeogr. Palaeoclimatol. Palaeoecol. 295, 281–292.

Suchéras-marx, B., Guihou, A., Giraud, F., Lécuyer, C., Allemand, P., Pittet, B., Mattioli, E., 2012. Impact of the Middle Jurassic diversification of Watznaueria (coccolith-bearing algae) on the carbon cycle and $\delta^{13}C$ of bulk marine carbonates. Glob. Planet. Chang. 86–87, 92–100.

Suchéras-Marx, B., Mattioli, E., Giraud, F., Escarguel, G., 2015. Paleoenvironmental and paleobiological origins of coccolithophorid genus *Watznaueria* emergence during the late Aalenian-early Bajocian. Paleobiology 41, 415–435.

Tiraboschi, D., Erba, E., 2010. Calcareous nannofossil biostratigraphy (Upper Bajocian–Lower Bathonian) of the Ravin du Bès section (Bas Auran, Subalpine Basin, SE France): Evolutionary trends of *Watznaueria barnesiae* and new findings of "*Rucinolithus*" morphotypes. Geobios 43, 59–76.

van de Schootbrugge, B., Bailey, T.R., Rosenthal, Y., Katz, M.E., Wright, J.D., Miller, K.G., Feist Burkhardt, S., Falkowski, P.G., 2005. Early Jurassic climate change and the radiation of organic walled phytoplankton in the Tethys Ocean. Paleobiology 31, 73–97.

van de Schootbrugge, B., Richoz, S., Pross, J., Luppold, F.W., Hunze, S., Wonik, T., Blau, J., Meister, C., van der Weijst, C.M.H., Suan, G., Fraguas, A., Fiebig, J., Herrle, J.O., Guex, J., Little, C.T.S., Wignall, P.B., Püttmann, W., Oschmann, W., 2018. The Schandelah Scientific Drilling Project: a 25-million year record of Early Jurassic palaeoenvironmental change from northern Germany. Newsl. Stratigr. https://doi.org/10.1127/nos/2018/0259.

Wang, F., Zhou, X.-H., Zhang, L.-C., Ying, J.-F., Zhang, Y.-T., Wu, F.-Y., Zhu, R.-X., 2006. Late Mesozoic volcanism in the Great Xing'an Range (NE China): timing and implications for the dynamic setting of NE Asia. Earth Planet. Sci. Lett. 251, 179–198.

Wiggan, N.J., Riding, J.B., Fensome, R.A., Mattioli, E., 2018. The Bajocian (Middle Jurassic): a key interval in the early Mesozoic phytoplankton radiation. Earth Sci. Rev. 180, 126–146.

Wignall, P.B., Newton, R.J., Little, C.T.S., 2005. The timing of paleoenvironmental change and cause-and-effect relationships during the early Jurassic mass extinction in Europe. Am. J. Sci. 305 (10), 1014–1032.

Zàk, K., Kost'ák, M., Man, O., Zakharov, V.A., Rogov, M.A., Pruner, P., Rohovec, J., Dzyuba, O.S., Mazuch, M., 2011. Comparison of carbonate C and O stable isotope records across the Jurassic/Cretaceous boundary in the Tethyan and Boreal Realms. Palaeogeogr. Palaeoclimatol. Palaeoecol. 299, 83–96.